

A Model for Wettability Alteration in Fractured Reservoirs

Pål Østebø Andersen, Steinar Evje, Hans Kleppe, and Svein Magne Skjæveland, University of Stavanger

Summary

We present a mathematical model for wettability alteration (WA) in fractured reservoirs. Flow in the reservoir is modeled by looking at a single fracture surrounded by matrix on both sides. Water is injected into the formation with a chemical component that enters the matrix and adsorbs onto the rock surface. These changes of the mineral surface are assumed to alter the wettability toward a more water-wet state, which leads to enhanced recovery by spontaneous imbibition. This can be viewed as a representation of “smart water” injection in which the ionic composition of injection brine affects recovery. The WA is described by shifting curves for relative permeability and capillary pressure from curves representing preferentially oil-wet (POW) conditions toward curves representing more-water-wet conditions. The numerical code was successfully compared with ECLIPSE for the specific case in which a fixed wetting state is assumed. Also, the relevance of the WA model was illustrated by modeling a spontaneous-imbibition experiment in which only a modification of the brine composition led to a change in oil recovery. The model can predict sensitivity to matrix properties such as wettability, permeability, and fracture spacing and to external parameters such as schedule of brine compositions and injection rate. Our model illustrates that one cannot use conventional reservoir modeling to capture accurately the behavior we observe. The rate of recovery and the level of recovery have a strong dependency on the component chemistry and its distribution. A significant feature of gradual WA by injecting a component is that the rate of fluid transfer is maintained between matrix and fracture. The resulting recovery profile after water breakthrough can behave close to linear as opposed to the square-root-of-time profile that is observed when the wetting state is fixed (Rangel-German and Kovscek 2002). The water will typically break through early as dictated by the initial POW state, but a higher final recovery will be obtained because higher saturations can imbibe. Improved understanding of the coupling between WA controlled by water/rock chemistry and fracture/matrix flow is highly relevant for gaining more insight into recovery from naturally fractured reservoirs.

Introduction

Carbonate reservoirs contain 60% of the worldwide oil reserves (Akbar et al. 2001), and many are naturally fractured. In naturally fractured reservoirs (NFRs), it is essential to mobilize the matrix oil to gain substantial recovery (Salimi and Bruining 2011). Injecting water will not displace oil as effectively as in conventional reservoirs because the advective flow is concentrated to fracture networks. A key recovery mechanism in such reservoirs is spontaneous imbibition (SI) of the injected fluid with (typically) countercurrent (CC) flow of oil back into the fracture network for advective transport. The wettability of the matrix rock is an important characteristic that defines to what extent water can be drawn into the rock [preferentially water-wet (PWW) rock] or if the rock rather retains the oil [preferentially oil-wet (POW) rock] (Zhou et al. 2000; Hirasaki and Zhang 2004). When the rock is more oil-wet or mixed-wet, the SI mechanism is slow and will not

lead to substantial recovery. Extensive studies on reservoir core samples have shown that most carbonates (80 to 90%) tend to be oil-wet or intermediate wet (Treiber and Owens 1972; Chilingar and Yen 1983; Cuiec 1984). To improve oil recovery, one should improve gravity drainage, alter the wettability toward water-wet, or enhance advection. A vast amount of imbibition experiments has been performed in which the composition of the initial or imbibing brine was varied (Zhang and Austad 2006; Zhang et al. 2007; Fathi et al. 2010, 2011). This demonstrated an effect on oil recovery by SI that one can explain by a wettability alteration (WA). By altering the concentration of naturally occurring ions in seawater, it is possible to imbibe higher saturations of water. Seawater is an available and inexpensive injectant for offshore field application. One can also apply surfactants to oil-wet carbonates to alter wettability (improving recovery by SI) and reduce surface tension (promotes recovery by gravity drainage) (Hirasaki and Zhang 2004; Bourbiaux 2009; Gupta and Mohanty 2011). Other suggested alternatives are heated injection fluids (Rao 1999; Al-Hadhrami and Blunt 2001) and nanofluids (Karimi et al. 2012). For a geological description of carbonate reservoirs, we refer to Roehl and Choquette (1985), Nelson (2001), and Ahr (2008).

Water injection into NFRs occurs under quite different conditions from those met in the laboratory. The matrix blocks are of highly varying size and are not fully surrounded by water until sometime after the water front has passed and imbibition has already started. Especially, the fully saturated boundary condition found in the laboratory may not generally be assumed in the field. Large matrix blocks may be exposed to water in the lower part and oil in the top part (caused by gravitationally segregated flow in the fractures). This situation favors cocurrent (COC) SI (Bourbiaux and Kalaydjian 1990; Pooladi-Darvish and Firoozabadi 2000a; Haugen et al. 2014). Depending on degree of exposure to one or two phases and the relative importance of gravity to capillary forces, the flow is a combination of COC and CC (Bourbiaux and Kalaydjian 1990). Chemical reactions and mixing will alter the fluid composition, and the water imbibing near the injector is different from the water imbibing farther into the reservoir. To gain better understanding of dynamic wetting changes in NFRs, it is useful to make a simplified representation containing some key features: (i) two-phase flow in a 1D+1D fracture/matrix geometry and (ii) WA resulting from a simplified reaction chemistry.

Such a simplified study is the aim of this article. We consider an NFR as modeled by a linear fracture surrounded by matrix on both sides. We assume advective flow in the fracture from an injector to a producer, with CC SI along the matrix interacting with the fracture flow. A component in the injected fluid can diffuse into the matrix, adsorb on the rock, and alter the wettability toward a more water-wet state, depending on the degree of adsorption. We name the component a WA agent. This is similar to a “smart water” injection in which ionic interactions between brine and rock surface are believed to alter the wetting state. The WA is represented by shifting relative permeability and capillary pressure curves from POW toward PWW with consistent sets found in the literature (Behbahani and Blunt 2004). CC SI in the matrix is described by a nonlinear diffusion equation, whereas advective transport in the fracture is described by standard Buckley-Leverett formulation. With this model, we can gain a better understanding of the interplay between advection, imbibition, reactive flow, and dynamic wettability. It also gives an indication of how results obtained in the laboratory can appear on a larger scale when the boundary conditions are dynamic.

Copyright © 2015 Society of Petroleum Engineers

This paper (SPE 174555) was revised for publication from paper IPTC 16957, first presented at the International Petroleum Technology Conference, Beijing, 26–28 March 2013. Original manuscript received for review 8 April 2013. Revised manuscript received for review 27 February 2015. Paper peer approved 8 April 2015.

The paper is organized as follows: A brief summary of relevant previous work is presented. Next, we present the mathematical formulation of the model. The model is tested in two ways: (i) by comparison with a commercial simulator and (ii) by an illustration of how one can use WA to match brine-dependent experimental data. The purpose of (i) is to verify that the 1D+1D model behaves similar to a full 2D model. The behavior of the model for different conditions is then explored by a series of numerical examples, followed by conclusions.

Previous Experimental Work

Much experimental work has been carried out to improve recovery from oil-wet and mixed-wet fractured reservoirs. Gravity drainage is an omnipresent mechanism, but for tight oil-wet rocks, the strong capillary forces retain much of the oil and the process is slow. Several studies have shown that recovery by spontaneous imbibition (SI) is improved when wettability turns toward water-wet (Anderson 1987; Zhou et al. 2000; Strand et al. 2006). The combined effect of fracture flow and wettability was demonstrated in the work of Graue et al. (2001) and Haugen et al. (2007, 2008, 2010). Blocks of porous media with defined fracture surfaces were flooded with water, and the impact of wettability was demonstrated by imbibition of water into the water-wet blocks and negligible imbibition into the oil-wet blocks as observed with magnetic-resonance-imaging techniques. Also, by flooding the individual blocks, they illustrated that one can obtain high recovery by advective displacement in an oil-wet medium, in contrast to the low recovery obtained by SI. Pooladi-Darvish and Firoozabadi (2000b) considered a setup of water-wet matrix blocks (both chalk and sandstone) with a narrow fracture network (0.5% pore volume). Water was injected at the bottom and imbibed into the blocks. A rising water level in the fractures displaced oil upward. They observed that blocks mainly experienced cocurrent (COC) production while having contact with oil, and countercurrent (CC) production when the blocks became fully immersed by brine as visualized by oil droplets rising beneath the water level in the fractures. At the transitions from COC to CC flow, oil production would be less efficient. This was in agreement with other experiments and modeling (Bourbiaux and Kalaydjian 1990; Pooladi-Darvish and Firoozabadi 2000a; Bourbiaux 2009).

The application of surface-active agents can alter wettability. Gupta and Mohanty (2011) measured oil/water contact angles on calcite plates and noted that optimal salinities and surfactant concentrations exist (in which the contact angle reaches a minimum). Xie et al. (2005) performed SI experiments on numerous reservoir cores with formation brine followed by surfactant solutions, and they observed increased recovery (5 to 10%). The additional recovery was ascribed in large extent to wettability alteration, rather than buoyancy. Surfactant was combined with various sulfate concentrations to imbibe into outcrop chalk (Strand et al. 2003). More sulfate led to increased recovery. Hirasaki and Zhang (2004) showed that the potential-determining ions CO_3^{2-} and HCO_3^- can make a carbonate surface negatively charged and water-wet. They combined sodium carbonate with surfactant to both alter wettability and reduce capillary forces. Because they obtained ultralow interfacial tension (IFT), the recovery was mainly driven by buoyancy. Zhang and Austad (2006) and Zhang et al. (2007) showed that simply modifying the setup of the natural ions in seawater (no surfactant) can have significant impact on the oil recovery. Sulfate, calcium, and magnesium are potential-determining ions toward chalk and can adsorb on the surface. It was suggested that adsorption of the negative sulfate ion reduces the positive charge of the chalk surface and releases negatively charged carboxyl groups in the oleic phase, which, in effect, make the surface more water-wet. The cations can then substitute oleic complexes near the surface. Cations also reduce the activity of sulfate by aqueous complexation that prevents scaling of anhydrite. Negligible variations in IFT are reported. Further studies (Fathi et al. 2010, 2011) showed that removing inert ions in seawater (sodium, chloride) also improves SI. It was proposed that the mechanism was related to improved surface access for the potential-determining ions. A study by Fernø

et al. (2011) investigated the sulfate effect for different mineralogies and initial wetting states.

In Strand et al. (2006), the adsorption properties of sulfate to chalk were used as a means to measure wettability by comparing the amount of adsorption compared with that of a completely water-wet sample. In Ahsan et al. (2012), long-term imbibition tests with porous disk showed that sulfate alone (at high concentrations) can improve wettability. Seawater injection into the North Sea field Ekofisk has caused subsidence (Agarwal et al. 2000). It is known that seawater and similar brines can dissolve and weaken chalk (Austad et al. 2008), but sulfate adsorption even by itself has been related to the weakening of the chalk matrix (Megawati et al. 2012). It was shown in Hiorth et al. (2010) that observed oil recovery by SI of seawater-like brines found in the literature correlates well with the calculated dissolution of chalk at high temperature. One should consider the chemical nature of seawater and its potential ability to alter wettability and weaken carbonate (especially chalk) during development of fractured carbonates.

Previous Modeling

Countercurrent (CC) spontaneous imbibition (SI) is normally represented by a nonlinear diffusion equation. Despite this simple nature, finding a proper time scale for recovery has been an ongoing topic to understand the role of different parameters and to upscale laboratory experiments to the field. The effect of static parameters (porosity ϕ , permeability K , interfacial tension σ , and characteristic length L) is well agreed upon, as illustrated by the correlation from Ma et al. (1997) for dimensionless time, as follows:

$$t_d = \frac{1}{L^2} \sqrt{\frac{K}{\phi}} \frac{\sigma}{\sqrt{\mu_w \mu_o}} t. \dots \dots \dots (1)$$

Changes in dynamic properties such as viscosity, relative permeabilities, and capillary pressure were harder to predict, resulting in different formulations (Mattax and KYTE 1962; Ma et al. 1997; Zhou et al. 2002; Tavassoli et al. 2005; Li 2007), valid under various restrictions. As demonstrated experimentally in Zhou et al. (2000), wettability can affect recovery time scales by orders of magnitude. General analytical solutions for 1D SI into a porous medium were derived in McWhorter and Sunada (1990), accounting for arbitrary flow parameters. The solution was used to make a universal scaling and was applied on a variety of imbibition experiments in Schmid and Geiger (2012, 2013). The mentioned analytical solutions are valid only until a no-flow boundary is encountered. Some papers (Tavassoli et al. 2005; Mirzaei-Paiaman et al. 2011) present simplified analytical solutions for imbibition that satisfy the boundary conditions and the average intake of water for all times, but not all conditions on the inner phase distribution. Cai et al. (2014) made a model that could account for tortuosity and gravity. Their model had several other imbibition models as special cases, but assumed piston-like fluid displacement.

Different models exist on the topic of brine-dependent SI. In Yu et al. (2008, 2009), a 1D model of SI core experiments was considered in which an adsorbing agent altered the wettability toward more water-wet and hence increased the recovery. The alteration process was matched by an appropriate adsorption isotherm. Similar models (Evje and Hiorth 2011; Andersen and Evje 2012a) with a more-consistent geochemical description [i.e., reaction kinetics matched from flooding experiments (Andersen et al. 2012)], correlated geochemically induced modifications of the matrix to changes in wettability and were matched against experimentally observed oil recovery. A geochemical model (Qiao et al. 2014) related surface complex formation (between species in the solid and fluid phases) to wettability. They used the model to explain the variation in SI oil recovery from chalk caused by different salinity and sulfate concentration. At low salinity and high sulfate concentration, it followed from equilibrium calculations that a lower amount of polar oil components stays attached to the surface.

Stoll et al. (2008) made an evaluation concerning the time scale of recovery driven by wettability alteration (WA). The authors

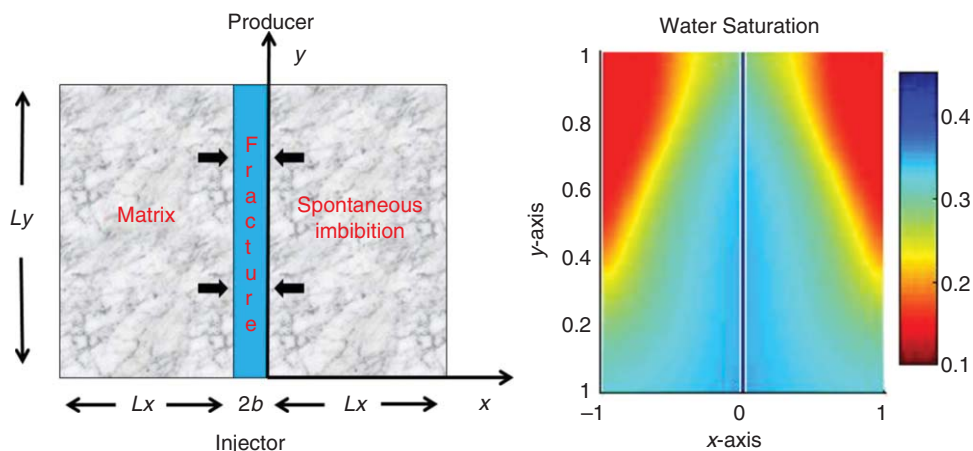


Fig. 1—Coordinate system for the reservoir (left). Advection occurs along fracture from injector to producer, whereas CC SI occurs along matrix toward the fracture. Water distribution after flooding 0.5 reservoir pore volumes of water is illustrated for the reference case (right).

showed that, in absence of significant capillary imbibition (oil-wet media), the imbibition rate was limited by molecular diffusion and could be 1,000 times slower than for the corresponding water-wet media. Scaling up experiments to meter-sized blocks indicated that the large time scales would be economically uninteresting. Bourbiaux et al. (2014) made similar observations, but further showed that pressure gradients of similar order, as observed in the fracture network, could significantly accelerate this process.

Models for fracture/matrix flow must account for the fact that imbibition is limited by the gradual advance of water in the fractures. Especially, the matrix boundary experiences a varying, not constant, saturation. There exist different model types depending on scale and complexity. De Swaan (1978) presented an analytical model for horizontal fracture/matrix flow in which a rate for fully saturated boundary (as given by an exponential expression) was incorporated in an imbibition source term with a convolution integral, thus accounting for varying fracture saturations. In Gautam and Mohanty (2004), the authors modeled an experimental setup in which water would flow in a thin channel (fracture) between two core plugs and oil was recovered from the cores by CC SI. Rangel-German and Kovscek (2002) presented experimentally how water flowing through a fracture imbibe to a surrounding matrix and presented an analytical solution for the combined matrix/fracture flow by extending a 1D solution for SI. The main assumption was that the capillary-diffusion coefficient (CDC) was constant. The authors showed how the initial recovery would be linear with time and later be linear with the square root of time, consistent with experimental behavior. A similar model concerning solute transport in one phase along a fracture was given in Mainguy and Ulm (2001). The solute was distributed by molecular diffusion and chemical dissolution/precipitation in the matrix. The authors gave an analytical expression for the long-term behavior of the solute front. Simplified models were considered for upscaling laboratory results to field in Aronofsky et al. (1958) and Mattax and Kyte (1962) by looking at recovery from vertically stacked blocks at a rising water level in the fractures. Pooladi-Darvish and Firoozabadi (2000b) made a simple analytical solution for 1D CC SI assuming a constant CDC. The solution incorporated that early-time recovery is proportional to \sqrt{t}/L , and showed that late-time recovery is represented by an exponential form, as suggested in Aronofsky et al. (1958). The solution was verified against CC SI experiments. It was then extended to vertical fracture flow and verified against experiments dominated by CC SI. Terez and Firoozabadi (1999) made a Buckley-Leverett-type model with a source term for the vertical fracture saturation profile. They proposed that two exponential terms (and time scales) should be used to incorporate cocurrent and CC SI. The model was compared with experiments in Pooladi-Darvish and Firoozabadi (2000b) in addition to new tests they performed of similar nature.

Reservoir-scale modeling of fractured reservoirs is usually performed with a multiphase dual-porosity formulation (Kazemi et al. 1976) in which the reservoir is assumed to contain matrix blocks separated by a fracture network. Recovery of oil from the blocks to the fractures is modeled by a transfer term. An interesting alternative to this approach was discussed in Unsal et al. (2010) in which the fracture network was modeled explicitly, whereas the matrix was included by means of source terms. That paper also contains several references for matrix/fracture flow models. Another approach called the multirate dual-porosity model was discussed in Geiger et al. (2013) in which the size distribution of matrix blocks was taken into account. This feature is important because the block size determines the time scale required for SI. Salimi and Bruining (2011) explored the effects of the Péclet number and gravity number on oil recovery in a reservoir-simulation study. In Delshad et al. (2009), the 3D compositional simulator UTCHEM was applied with a dynamic wettability option to simulate WA by surfactant injection into fractured reservoirs.

A previous paper on the model discussed in this paper is given in Andersen and Evje (2012b). In that paper, the model was considered at fixed wettability without component transport, and the key model parameters were discussed. A dimensionless number was proposed to evaluate the efficiency of waterflooding through a fracture/matrix system.

System Description and Modeling

We will consider a geometry given by a fracture surrounded symmetrically by matrix rock, as shown in Fig. 1. The system we consider contains two immiscible liquid phases, namely oil (o) and water (w). The water phase can carry a component that we term a wettability-alteration (WA) agent because we assume this component has the potential to interact with the matrix and affect wettability properties. Other main assumptions we will use are

- The rock and fluids are incompressible.
- The fracture and matrix are separate regions with different flow properties.
- Each region has constant permeability, porosity, and width. The saturation functions (capillary pressure and relative permeability) are also regionally distinct.
- WA chemistry occurs instantaneously.
- The WA is coupled to adsorption of the WA agent and is represented by shifting relative permeability and capillary pressure functions. Viscosities and interfacial tension (IFT) are assumed constant.
- Advective flow occurs only in the fracture in the y -direction. Dispersion effects are negligible in the fracture flow.
- Capillary flow in the matrix occurs only along the x -direction, in countercurrent (CC) manner.

- Gravity effects are not considered; thus, we ignore gravity drainage and water-level rise in the fractures.

We will now give a mathematical description of the model. Consider a horizontal plane (x, y) such that the y -axis runs parallel with a linear fracture of length L_y and width $2b$. The fracture cuts the plane in half, and porous medium (matrix region) is on either side going a length of L_x on either side of the fracture [the geometry and notation are inspired by Mainguy and Ulm (2001)]; see Fig. 1.

The fracture and matrix domains are given by

$$\begin{aligned}\Omega^f &= [(x, y) : -2b < x < 0; 0 \leq y \leq L_y], \\ \Omega^m &= [(x, y) : -2b - L_x < x < -2b, 0 < x < L_x; 0 \leq y \leq L_y]. \\ &\dots\dots\dots (2)\end{aligned}$$

The injector and producer are at the surfaces:

$$\begin{aligned}\Gamma^{\text{inj}} &= [(x, y) : -2b < x < 0, y = 0], \\ \Gamma^{\text{prod}} &= [(x, y) : -2b < x < 0; y = L_y]. \dots\dots\dots (3)\end{aligned}$$

Relevant local variables are phase pressures p_w and p_o , phase saturations S_w and S_o , and WA-agent concentration in the water phase, c . We make use of the following constraints:

- The saturations are dependent as $S_o + S_w = 1$. From this, we eliminate the oil saturation S_o .
- The phase pressures p_w and p_o are in local equilibrium as given by the capillary pressure, P_c , which is a known function, $p_o - p_w = P_c(S_w)$. This is used to eliminate the water-phase pressure p_w .
- From boundary conditions, we can determine the total velocity at any position. This parameter will replace the oil-phase pressure p_o .

Accordingly, the final model will be expressed by the two variables water saturation S_w and WA-agent concentration c . Define phase mobilities for matrix and fracture as

$$\lambda_j^m(S_w, c) = \frac{k_{rj}^m(S_w, c)}{\mu_j}, \quad \lambda_j^f(S_w) = \frac{k_{rj}^f(S_w)}{\mu_j}, \dots\dots\dots (4)$$

and water fractional-flow functions as

$$f_w^m(S_w, c) = \frac{\lambda_w^m}{\lambda_w^m + \lambda_o^m}, \quad f_w^f(S_w) = \frac{\lambda_w^f}{\lambda_w^f + \lambda_o^f}. \dots\dots\dots (5)$$

The index j refers to oil (o) or water (w) phase, whereas m and f refer to matrix and fracture, respectively; k_{rj} is relative permeability; and μ_j is viscosity. The matrix relative permeabilities k_{rj}^m and capillary pressure curves P_c^m are functions of both water saturation S_w and concentration c because the WA agent can alter the functions by changing the matrix wettability. The WA agent is, however, assumed to behave inertly in the fracture. In other words, this study focuses on a situation in which the change in spontaneous-imbibition (SI) behavior caused by the spreading of a chemical component into the matrix is the central issue. A next step would be to implement effects of WA in the fracture also.

Transport equations for the matrix are given in Eq. 6. One can derive them with an approach similar to that in Yu et al. (2008). The water-phase flow is controlled by capillary pressure gradients. The WA agent flows along with the water phase, but also spreads by dispersion/diffusion and retains by adsorption:

$$\begin{aligned}\phi^m \partial_t S_w &= -\partial_x [K^m \lambda_o^m(S_w, c) f_w^m(S_w, c) \partial_x P_c^m(S_w, c)] \\ \phi^m \partial_t [S_w c + A(c)] &= -\partial_x [K^m \lambda_o^m(S_w, c) f_w^m(S_w, c) c \partial_x P_c^m(S_w, c)] \\ &\quad + \phi^m \partial_x [S_w D^m (v_w^m) \partial_x c] \\ (x, y) &\in \Omega^m \dots\dots\dots (6)\end{aligned}$$

Matrix porosity ϕ^m and absolute permeability K^m are constant. $A(c)$ represents the adsorbed component. Flow in the fracture (Eq. 7) is controlled by an advective term as a result of injection. In

addition, source terms relate the fracture flow with flow in the matrix:

$$\begin{aligned}\phi^f \partial_t S_w + \phi^f v_T^f(t) \partial_y [f_w^f(S_w)] \\ = -\frac{1}{b} [K \lambda_o(S_w, c) f_w(S_w, c) \partial_x P_c(S_w, c)] |_{\{x=0^+\}} \\ \phi^f \partial_t (S_w c) + \phi^f v_T^f(t) \partial_y [f_w^f(S_w) c] \\ = -\frac{1}{b} [K \lambda_o(S_w, c) f_w(S_w, c) c \partial_x P_c(S_w, c)] |_{\{x=0^+\}} \\ \quad + \frac{1}{b} [\phi S_w D(v_w) \partial_x c] |_{\{x=0^+\}} \\ (x, y) \in \Omega^f \dots\dots\dots (7)\end{aligned}$$

We work with average values in the fracture, meaning that these variables depend on (y, t) , but not x . The source terms are evaluated by properties of both fracture and matrix. The fracture width $2b$ and fracture porosity ϕ^f are assumed constant; v_T^f is the total pore velocity in the fracture. It is uniform along the fracture, but can vary in time as defined by injection conditions. Finally, we note that the matrix water velocity v_w appearing in the dispersion coefficient D is given by

$$v_w^m = \lambda_o^m f_w^m K^m \partial_x P_c^m. \dots\dots\dots (8)$$

Relative Permeability and Capillary Pressure Functions. In this subsection, we present expressions for relative permeability curves (k_{ro}, k_{rw}) and scaled capillary pressure curves J . For the matrix, we will consider two consistent sets of mixed-wet curves, qualitatively representing either preferentially water-wet (PWW) ($k_{ro}^{m,pww}, k_{rw}^{m,pww}; J^{m,pww}$) or preferentially oil-wet (POW) ($k_{ro}^{m,pow}, k_{rw}^{m,pow}; J^{m,pow}$) state as functions of water saturation. We then include the wettability dependence as an interpolation between the curves. The fracture is represented by the set $(k_{ro}^f, k_{rw}^f; J^f)$.

Fixed Wettabilities. We introduce the normalized water saturation $S^* = \frac{S_w - S_{wc}}{1 - S_{or} - S_{wc}}$, where S_{wc} represents the connate water saturation and S_{or} the residual oil saturation at which the oil phase does not flow. Relative permeabilities are modeled with LET-correlations (Lomeland et al. 2005):

$$\begin{aligned}k_{rw}(S_w) &= k_w^* \frac{(S^*)^{L_w}}{(S^*)^{L_w} + E_w (1 - S^*)^{T_w}}, \\ k_{ro}(S_w) &= k_o^* \frac{(1 - S^*)^{L_o}}{(1 - S^*)^{L_o} + E_o (S^*)^{T_o}} \dots\dots\dots (9)\end{aligned}$$

for $S_{wc} < S_w < 1 - S_{or}$. L_w, E_w, T_w, L_o, E_o , and T_o represent shape parameters, whereas k_w^* and k_o^* are endpoint relative permeability values. Separate curves are defined by specifying different parameters.

As a model for capillary pressure, we consider a dimensionless scaled function J of the following form $P_c(S^*) = P_{c,\text{ref}} J(S^*)$, where variations in rock properties (ϕ, K) and IFT (σ) can be incorporated as $P_{c,\text{ref}} = \sigma \sqrt{\frac{\phi}{K}}$ (Dullien 1992). For the matrix, we let imbibition curves J^m be defined as

$$\begin{aligned}J^m(S_w) &= \frac{a_1(A_m, B_m)}{1 + k_1 S^*} - \frac{a_2(A_m, B_m)}{1 + k_2 (1 - S^*)} + b_1, \\ J^m(S_w = S_{wc}) &= A_m, \quad J^m(S_w = 1 - S_{or}) = B_m. \dots\dots (10)\end{aligned}$$

See Skjaeveland et al. (2000) for a similar correlation. For preferentially oil-wet (POW) or preferentially water-wet (PWW) matrix, we choose parameters A_m, B_m, b_1, k_1 , and k_2 in accordance with the characteristic shape of experimental capillary pressure data. The a_1 and a_2 are constrained by the fixed boundary conditions in (Eq. 10). J^m will decrease with S^* and be bounded to the interval $B_m < J^m < A_m$. The fracture is assigned Corey relative permeabilities, as shown next:

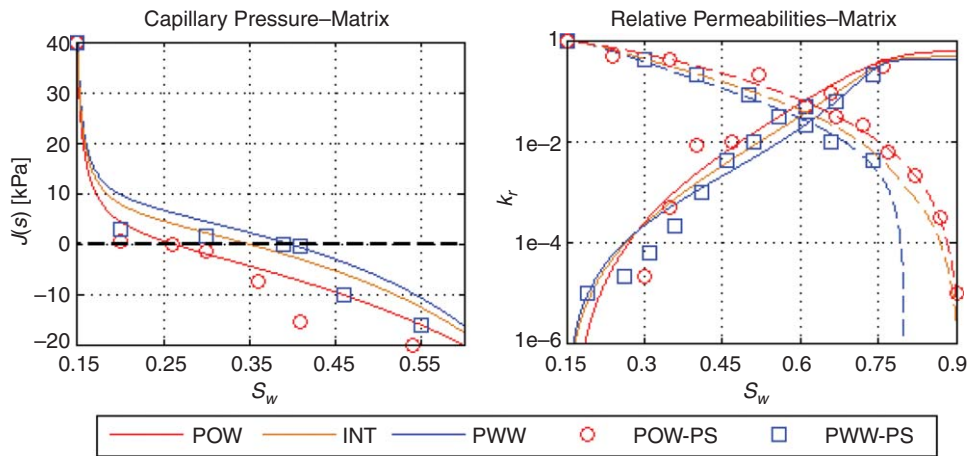


Fig. 2—Capillary pressure (left) and relative permeability (middle) curves in the fracture and relative adsorption isotherm (right) for the WA agent.

$$k_{rw}^f(S_w) = S_w^{n_f}, \quad k_{ro}^f(S_w) = (1 - S_w)^{n_o} \quad (11)$$

The fracture capillary pressure is assumed, given by the following correlation:

$$J^f(S_w) = \frac{a_0(A_f, B_f)}{1 + k_0 S_w^*} + b_0(A_f, B_f), \quad J^f(0) = A_f, \quad J^f(1) = B_f \quad (12)$$

The use of nonzero capillary pressure and nonlinear relative permeabilities in fracture modeling has become more relevant in recent years. In Dejam and Hassanzadeh (2011), the authors state that formation of liquid bridges requires a nonzero capillary pressure in the fractures. In De La Porte et al. (2005), the authors calculated fracture capillary pressures and showed that the magnitude will increase with smaller aperture. They also illustrated that fracture relative permeabilities can become highly nonlinear because of the interplay of gravity, surface roughness, and aperture. Haugen et al. (2007) compared in-situ oil displacement obtained by magnetic resonance imaging with numerical simulations, and noted that some features could only be matched with a varying-fracture capillary pressure.

Altering Wettabilities. We couple the alteration in wettability to the adsorption of WA agent on the matrix surface. The amount of adsorbed species (measured per porous volume) is assumed to be given by a Langmuir isotherm (see Remark 2 in the following):

$$A(c) = A_{\max} \frac{rc}{1 + rc} \quad (13)$$

This implies that more WA agent will adsorb if the concentration is increased, but not more than the threshold A_{\max} . The WA is coupled to the relative adsorption $w(c) = \frac{A(c)}{A_{\max}}$ —that is, how much is adsorbed compared with what is obtainable. An illustration of this scaled isotherm, w , is given in Fig. 2. The interpolation is assumed to be linear in w :

$$\begin{aligned} k_{rw}(S_w, c) &= w(c)k_{rw}^{pww}(S_w) + [1 - w(c)]k_{rw}^{pow}(S_w), \\ k_{ro}(S_w, c) &= w(c)k_{ro}^{pww}(S_w) + [1 - w(c)]k_{ro}^{pow}(S_w), \\ J(S_w, c) &= w(c)J^{pww}(S_w) + [1 - w(c)]J^{pow}(S_w). \end{aligned} \quad (14)$$

If there is no adsorbed WA agent, then no WA has occurred, and the matrix remains POW. Then $w=0$ and the curves are given by the POW state. On the other hand, if the matrix has adsorbed its maximal amount of WA agent, the matrix becomes PWW. Then $w=1$, and the curves are given by the PWW state.

- Remark 1: The adsorption of a component can depend on electrical forces interacting with the charged matrix surfaces. The pH of the brine and ionic capacity of the surface are of high importance; see Appelo and Postma (2005). Isotherms are simplified approaches to capture the retention of a species across the range of relevant concentrations. As shown in Megawati et al. (2012), increased concentrations do not increase the adsorption of sulfate after a certain point. It has also been shown that sulfate adsorbs and desorbs on chalk reversibly (Strand et al. 2006). A Langmuir isotherm captures both features. Similarly, Langmuir-type adsorption was applied for surfactants (Bourbiaux et al. 2014)
- Remark 2: WA occurs at the microlevel by a modification of IFTs. These changes affect the saturation curves that are measured on the macroscale. The linear interpolation between wettability states, as given by Eq. 14, assumes that the wettability transformation occurs instantaneously and that the wettability state is linearly related to the adsorption. To get a more-accurate (nonlinear) relation, one can measure wettability curves for a given oil/water/rock system at several brine concentrations. This was demonstrated in Ahsan et al. (2012). By considering spontaneous imbibition (SI) experiments and the recovery behavior, one can estimate the time scale of brine-chemistry effects. In the work of Zhang and Austad (2006), it was seen that at increased sulfate concentration, high saturations imbibed during a couple of days.
- Remark 3: In this work, we consider different wetting states at the same initial saturation. Wetting state is strongly linked to initial water saturation: If a high saturation of oil invades the matrix, a larger fraction of the pores will be rendered oil-wet by adsorption of polar components; see also Zhou et al. (2000). Wettability is also linked to the chemical composition of the fluids: In Yu et al. (2007), it was shown that contact angles of oil droplets in brine measured on a mineral surface can become more water-wet when exposed to synthetic seawater rather than distilled water. In Ahsan et al. (2012), it was shown that cores aged with sulfate brines obtained a higher residual water saturation. We assume a situation in which the fluids are initially in equilibrium and a component enters through the water phase and affects the thermodynamic state. In terms of wetting change, one may observe this by a release of the oil film and a redistribution of the phases with more oil centrally in the pores. In other words, we consider differences in wetting state caused by changes in chemistry and not caused by changes in initial saturation.

Dispersion. The dispersion coefficient D^m is given by an advective and diffusive part (Appelo and Postma 2005):

Well spacing, L_y	500 m	Fracture pore velocity, v_T^f	250 m/d	Molecular diffusion coefficient, D_{mol}	$7 \cdot 10^{-10} \text{ m}^2/\text{s}$
Fracture aperture, $2b$	100 μm	Matrix permeability, K^m	5 md	Matrix dispersivity, α_{disp}^m	0.05 m
Fracture porosity, ϕ^f	1.0	Oil viscosity, μ_o	1 cp	Adsorption parameter, r	1.85
Matrix porosity, ϕ^m	0.20	Water viscosity, μ_w	1 cp	Maximum WA adsorption, A_{max}	0.5
Fracture spacing, $2L_x$	0.25 m	Reference capillary pressure, $P_{c,ref}$	1 kPa		

Table 1—Reference input parameters used for simulation studies.

$$D^m = \alpha_{disp}^m |v_w^m| + D_{mol}, \quad \dots \quad (15)$$

where α_{disp}^m (m) is the dispersivity of the medium, v_w^m the water pore velocity [see (Eq. 8)], and D_{mol} (m^2/s) the molecular diffusion coefficient of the species.

Initial and Boundary Conditions. In addition to the transport equations, the system is equipped with initial conditions of the following form:

$$S_w(x, y, t = 0) = S_{w,0}(x, y), \quad c(x, y, t = 0) = c_0(x, y). \quad \dots \quad (16)$$

Boundary conditions for the fracture at the injector are given by the composition of the injected fluid:

$$S_w(y = 0, t) = S_w^{inj}, \quad c(y = 0, t) = c^{inj}. \quad \dots \quad (17)$$

The boundary at the exterior of the matrix is assumed closed; that is,

$$\partial_x J^m(S_w, c)|_{(x=L_x, y)} = 0, \quad \partial_x c|_{(x=L_x, y)} = 0. \quad \dots \quad (18)$$

Finally, we note that the fracture matrix interface is defined by capillary pressure continuity (except when a phase is immobile) and concentration continuity:

$$J^m(S_w, c)|_{(x=0^+, y)} = J^f(S_w)|_{(x=0^-, y)}, \quad c|_{(x=0^+, y)} = c|_{(x=0^-, y)}. \quad \dots \quad (19)$$

The fracture source terms in Eq. 7 controlling flow between matrix and fracture are defined by continuity with the matrix fluxes given through Eq. 6. These interface conditions are in line with fracture-flow modeling in the literature; see Duijn et al. (1995) and Salimi and Bruining (2011).

Numerical Solution. The system is solved by an operator-splitting approach on the basis of making subsystems in which flow goes either in the x - or the y -direction and we switch between solving each system. The flow in x -direction is further split into capillary diffusion and component dispersion/diffusion. The system is discretized into $N_x = 25$ cells equally sized along the positive x -axis, and $N_y = 70$ equally sized cells along the y -axis; 100 splitting steps are made per injected fracture volume (FV). More information is found in Appendix A.

Numerical Investigations. Input. Reference-case input parameters are given in Table 1. In addition, we consider initial saturations $S_{w,0}^m = 0.15$ in the matrix and $S_{w,0}^f = 0.0$ in the fracture. Initial concentrations are $c_0 = 0.0$. Water is injected, so $S_w^{inj} = 1$. Also, the reference injected concentration is $c^{inj} = 1$. With the given parameters, we note that one reservoir pore volume (PV) (RPV) corresponds to 501 FV. Curves for capillary pressure and relative permeability are shown for fracture and matrix in Figs. 2 and 3, respectively (corresponding curve parameters are given in Tables 2 and 3).

The matrix curves are displayed for POW and PWW states. The curves are given by the correlations (Eq. 9 and Eq. 10) matched to data (also displayed) obtained from pore-scale network modeling (Behbahani and Blunt 2004) in which different wetting distributions were applied to match experimental SI and flooding data as given in Zhou et al. (2000). Especially, we apply the saturation data corresponding to aging times $t_a = 240$ hours for POW data, and $t_a = 48$ hours for PWW data; see Behbahani and Blunt (2004) (capillary pressures are adjusted to account for our choice of permeability). Also, an interpolation of the curves is displayed according to Eq. 14 to indicate how interaction with the WA agent might alter the wettability from POW toward PWW.

Behavior at Constant Wettability. First, we consider the extremes of the model. With the reference-case input data, we compare the model behavior if the matrix is uniformly and fixed POW or PWW. When the fracture is fully water-saturated, the capillary pressure is zero (see the green curve on the left in Fig. 3). Water

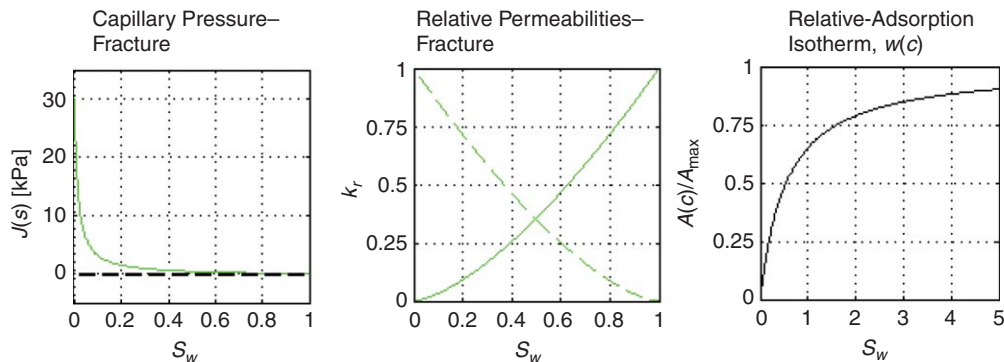


Fig. 3—Scaled capillary pressure J (left) and relative permeability $k_{r,o}$, $k_{r,w}$ (right) curves for the matrix at two mixed-wet states (POW and PWW) as fitted by correlations to pore-network simulation data (PS) provided in Behbahani and Blunt (2004). The interpolated (INT) curves correspond to the reference case with WA-agent concentration $c = 1$.

	S_{wr}	S_{or}	k_w^*	k_o^*	N_{kw}	N_{ko}	A_f	B_f	k_f
Fracture	0	0	1	1	1.5	1.5	30	0	75

Table 2—Fracture-curve parameters.

	S_{wc}	S_{or}	k_w^*	L_w	E_w	T_w	k_o^*	L_o	E_o	T_o	A	B	k_1	k_2	b_1
POW	0.15	0.09	0.6	3.5	15	2.5	1	2.5	2.5	1	35	-80	90	3	28
PWW	0.15	0.2	0.4	2	200	2.5	1	1.5	10	1.5	40	-80	100	5	24.8

Table 3—Matrix-curve parameters for POW and PWW states.

will spontaneously imbibe into the matrix until the same capillary pressure is obtained. Note, from the capillary pressure curves in Fig. 2, that, in the more=oil-wet case, the matrix water saturations will approach 0.26 because the capillary pressure vanishes at this saturation (the driving force requires a capillary pressure gradient; see Eq. 7). In the PWW case, the water saturations may reach 0.396. This corresponds to maximum recoveries of 13.1 and 29.1%, respectively; see Eq. 22. One can summarize these reference simulations as follows:

- Water breaks through first for the POW reservoir, as seen by a rise in the water flux after a short time (Fig. 4, left). The injected water flows preferentially through the fracture and imbibes slowly to the matrix.
- In the PWW case, water breakthrough does not occur until several FVs (approximately 1/10 RPV) are injected, indicating a more-efficient imbibition process. It is followed by a gradually increasing water flux, indicating that much of the injected water still goes into the matrix.

- At very early times, before water breakthrough, the recovery profiles are linear (Fig. 4, middle). The long-term recovery profiles are indicated in Fig. 4, right. Note that the time scale of recovery for the POW matrix is roughly an order of magnitude higher than that for the PWW matrix, as seen also on laboratory scale (Zhou et al. 2000).
- The distribution of water is shown in Fig. 5 after injecting 0.25 RPV. In accordance with the previous statements, the PWW matrix obtained higher saturations with deeper reach into the matrix compared with the POW matrix.

Numerical-Model Comparison. Our model (1D+1D) is tested numerically by comparison with the commercial simulator ECLIPSE-100 with constant-wettability cases POW and PWW. Identical grids are used for the 1D+1D model and ECLIPSE model. The ECLIPSE model is a 2D model (i.e., communication in both coordinate directions in matrix is allowed). Intrinsic fracture permeability was set according to Golf-Racht (1982):

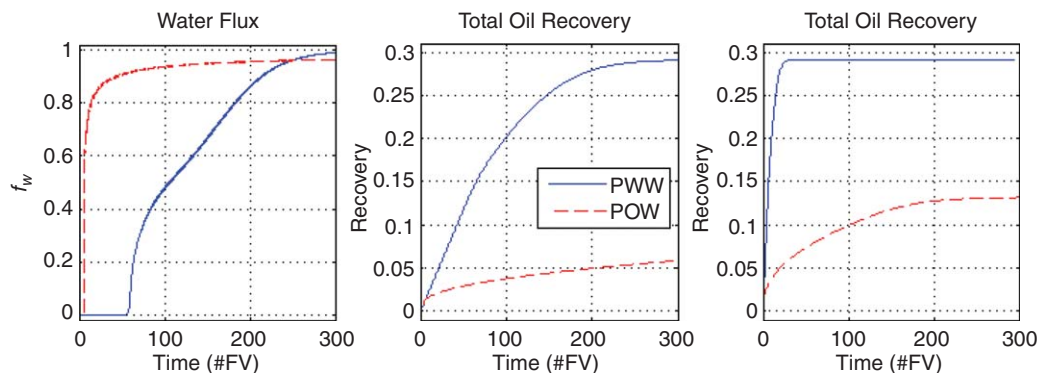


Fig. 4—Producer water flux (left) and oil recovery (middle and right) measured vs. scaled time (FV of water injected) for reference case with fixed wettability (either POW or PWW).

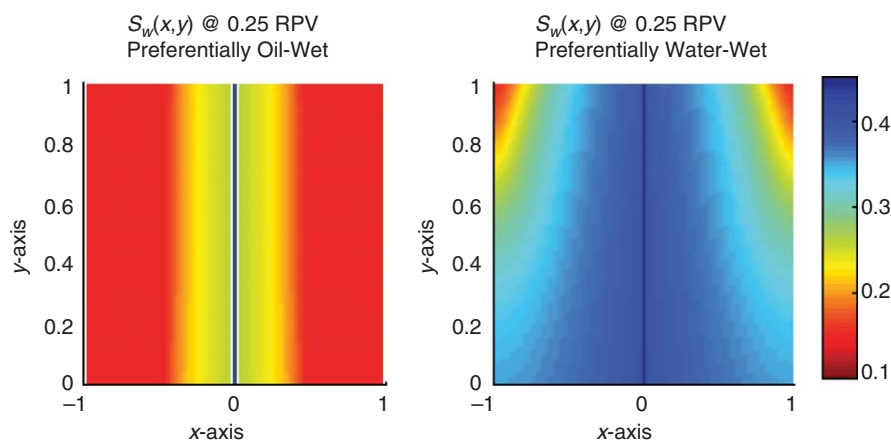


Fig. 5—Distribution of water in reservoir after having injected 0.25 RPV of water in reference case for fixed wetting state; POW (left) and PWW (right) matrix. The presented axes are scaled as x/L_x and y/L_y .

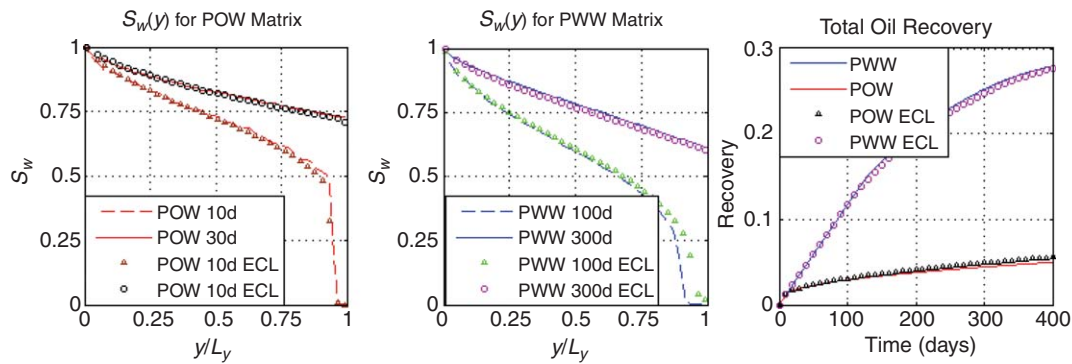


Fig. 6—Comparison of base-case simulation with ECLIPSE for two fixed wettability states (POW and PWW) showing saturation profiles along fracture (left for POW, middle for PWW) and recovery curves.

$$K^f = \frac{(2b)^2}{12} \approx 1,000D. \quad (20)$$

Both local behavior (given by fracture-saturation profiles in Fig. 6, left and middle) and overall behavior (given by recovery in Fig. 6, right) are well-captured.

Role of Block Size. The geometrical configuration of the reservoir can pose a challenge for water injection. The time scale of SI is proportional to the square of the block dimension; see (Eq. 1), which indicates that large blocks need a lot more time to be produced. As an example, consider the PWW case in which block dimension L_x is varied. To keep a fixed-injection rate, we vary the fracture velocity as $v_T^f \propto L_x$. Injecting a comparable amount of water (measured in reservoir volumes) is less efficient when the blocks are large; see Fig. 7. It was, however, noted (Bourbiaux 2009) that for very large blocks (10 to 100 m), CC gravity drainage can be a more-efficient mechanism than CC SI for strongly water-wet media.

Modeling Core SI Experiments. Also, we consider an SI experiment on chalk found in the literature (Zhang and Austad 2006) in which only the sulfate concentration in the imbibing brine (synthetic seawater) is varied from test to test, and the connate water contains no sulfate. The cores are cylindrically shaped with 6-cm length and 3.5-cm diameter. Initial saturation is $S_{w,0} = 0.25$. The linear 1D matrix model (Eq. 6) was implemented to simulate CC SI with sulfate adsorbing by Eq. 13 and dynamically altering saturation functions, as given by Eq. 14. The boundary condition at the core surface is similar to the boundary conditions of a matrix/fracture boundary: $J(0,t) = 0$, $S_w(0,t) = 1$, $c(0,t) = c_{imb}$. Two different wettability states and a Langmuir isotherm were selected to match the recovery profiles. The results are given in Fig. 8. The results indicate that WA, as dictated by sulfate adsorption, offers an explanation for the observed brine-dependent oil recovery, and it is a valid assumption to be used on a larger scale.

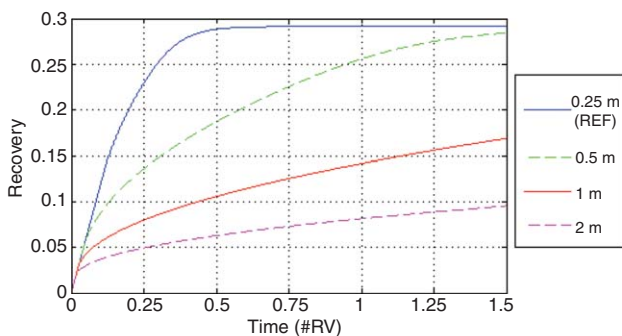


Fig. 7—Effect of block size on recovery for the PWW reference case at a given rate.

Injecting Different Concentrations of WA Agent. To study the interplay between WA (controlled by the WA agent) and matrix/fracture flow, we let the injected brine carry a certain concentration of the WA agent. As injection begins, the matrix is originally in a POW state. Several tests were run in which the injected concentration c^{inj} was varied. Results are shown in Figs. 9 and 10.

- When WA agent adsorbs on the matrix surface, the capillary pressure is raised, improving the potential for SI. A higher concentration of WA agent shifts the wettability more and therefore results in different end recoveries for different concentrations.
- The time scales are also shifted from that of the original state, POW, to that of the end state, PWW, as seen in Fig. 9 (right) in which it is seen that higher end recovery is obtained in shorter time. This is consistent with laboratory-scale brine-dependent SI data, as observed in Fathi et al. (2010, 2011).
- Early-time behavior is dominated by the initial wetting state. In all cases, the water breaks through at similar times (seen by the rise in water flux in Fig. 9, left), indicative of the initial wetting state, POW, of the matrix. The wettability changes occur behind the water front because the component must enter the matrix and react, whereas the frontal water only encounters unaltered areas. It is therefore reasonable that breakthrough times are not affected by the chemistry. This should also hold for more-general geometries.
- The distributions of water and component after 0.25 RPV are given in Fig. 10. Note that the component has only effectively entered half the matrix region (nearest the injector) at

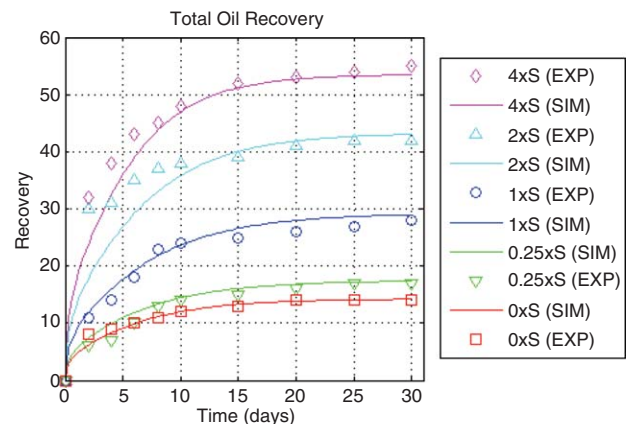


Fig. 8—SI experiments (EXP) from Zhang and Austad (2006) were history matched (SIM) with the matrix model (Eq. 6) with wettability alteration by Eq. 12 and Eq. 13 and fixed boundary conditions $J(0,t) = 0$, $S_w(0,t) = 1$, $c(0,t) = c_{amb}$. The recovery is affected by the SI brine composition, synthetic seawater with 0 to 4 times normal concentration of sulfate.

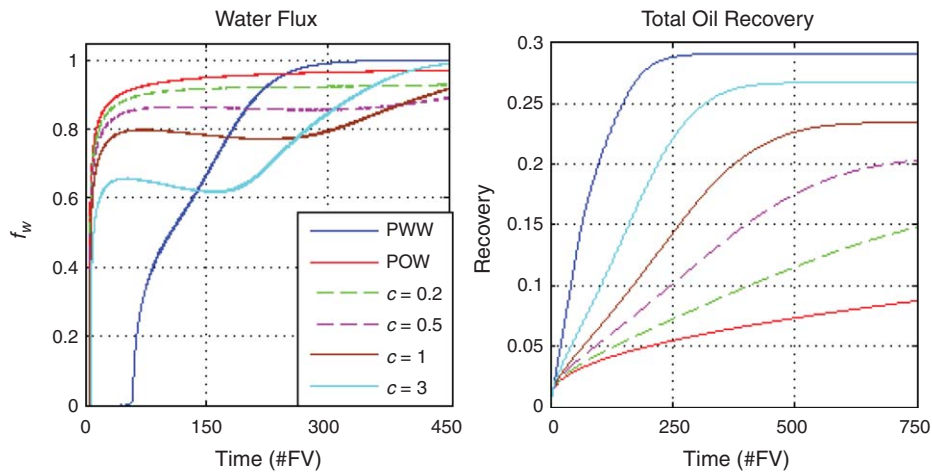


Fig. 9—Producer-water flux (left) and oil recovery (right) vs. time (FVs of water injected) for different injected concentrations of WA agent compared with fixed wetting states: POW and PWW.

this time. In this region, the water is spreading deeper into the matrix and to higher saturations. The region closer to the producer (unaffected by the WA agent) has a narrower imbibition depth with low saturations obtained, comparable with Fig. 5 (left).

- The impact of WA becomes apparent by a deviation from the POW reference case after a short time; see Fig. 9, left. A competition between lowered capillary pressure as saturations increase and increased capillary pressure by WA-agent adsorption leads to a more-stable matrix/fracture transfer rate. This is observed as a stabilization of the water flux during a long time of production and a very linear recovery profile. The onset and dominance of WA in the profile rely heavily on how efficiently the component is able to spread and to alter the wettability (to be discussed later). In general, a network of fractures should produce a more-advanced profile in which the linear vs. square-root regime predicted in this geometry may be less recognizable.
- The final stages of recovery are dominated by imbibition fronts hitting no-flow boundaries, and vanishing effects of chemistry resulting in reduced fluid transfer across the matrix/fracture boundary. The water flux steadily approaches unity as the potential oil is recovered.

It is important to be able to observe the effect of the injected component in the field as soon as possible. This may determine whether one should pursue or stop continued use of chemicals. As

explained, our model suggests that WA does not necessarily affect the breakthrough time, which is indicative of the initial state. The behavior after breakthrough should, however, be more indicative. This does, of course, depend on distribution and reactivity of the WA agent. A possible reason for seeing effects quickly (as in the examples) is the short residence time in the fracture network. Specifically, if the SI rate is low, injected water is produced quickly. A change in SI rate caused by chemical interaction will cause an impact on the flow pattern. This response is also transported quickly to the producer.

An additional comparison was made for the reference case $c = 1$ in which we distinguish between fixed wettability (corresponding to uniform and constant concentration) and a gradual WA in which WA agent is injected. The results are given in Fig. 11. When the initial wettability is more water-wet, a high SI rate starts immediately, resulting in a more-delayed water breakthrough than if the initial state was POW. The SI rate is then continuously reduced because of the weakening of the capillary pressure gradient. The water flux increases gradually until no more oil is produced. For varying wettability, we see early breakthrough followed by a stabilizing water-flux/linear-recovery profile. Note that the water flux in the varying case is lower than in the fixed case after some time, and at that time, produces oil faster than in the case of fixed wetting. The recovery curve however lags behind, and the total recovery period is longer.

In Fig. 12, we compare the outgoing flux of the WA agent ($f_w c$) with that of the water (f_w) for the reference case. The WA

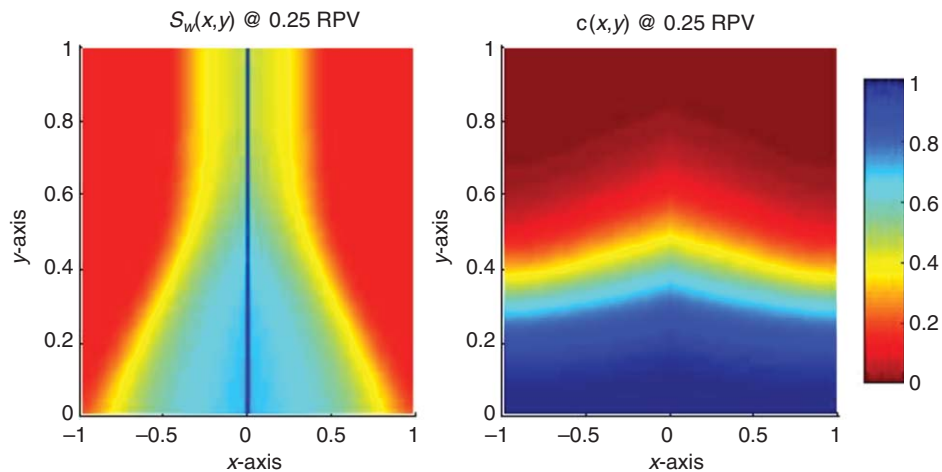


Fig. 10—Distributions of water saturation (left) and WA-agent concentration (right) after 0.25 RPV of brine was injected for the reference case ($c = 1$).

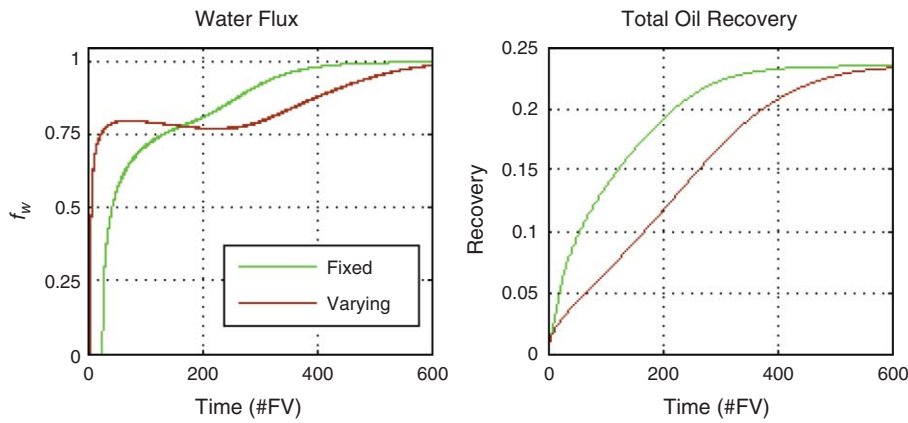


Fig. 11—Producer water flux and oil recovery vs. time (FVs of water injected) comparing gradual WA to fixed wettability for the reference case ($c = 1$).

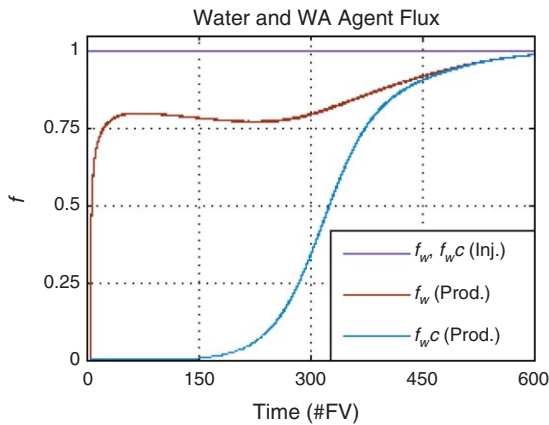


Fig. 12—Injected and produced fluxes of water and component f_w , $f_w c$ vs. time (FVs of water injected) for reference case ($c = 1$).

agent arrives later at the producer than the water because of the interaction with the matrix (the fracture is initially oil-saturated). The WA agent is diluted into the connate water in the matrix and adsorbs onto the matrix rock surface. This process effectively strips the water of WA agent, and as a result, there is no significant production of the component until approximately 0.5 RPV = 250 FV has been injected. Note that this event coincides well with the time when the water flux begins to increase again. At this point, the reservoir does not adsorb the component very efficiently because it partly is produced again on the other side. The matrix surface becomes saturated with the component at the given concentration and adsorbs less of the injected WA agent.

Therefore, the WA ceases and does not sustain the capillary drive. The SI process weakens, and recovery eventually stops.

Required Amount of Adsorption. When the WA agent adsorbs to the surface to change wettability, it is important to know how much species is required to achieve a certain effect. If several PVs of injection are needed to alter the wettability significantly, it may be an expensive option compared with other techniques. In Fig. 13, we have varied the parameter A_{max} (the amount that must adsorb for maximum WA) across a wide range. It is seen (Fig. 13, right) that oil recovery is delayed when A_{max} is high (the end recovery is the same). The increased adsorption means that more WA agent must be injected to reach the desired wettability changes. Because the matrix then has higher capacity to store the component, it will arrive later at the producer (Fig. 13, middle). If A_{max} is very small (compared with the injected concentration), it seems that the behavior converges toward the case with fixed wetting state (for $c = 1$). The wettability will change almost instantaneously at the front, and the water will lose negligible component by adsorption. The dilution of WA agent into the connate water will inhibit the alteration process and set the difference from the fixed wetting-state behavior. For low A_{max} , the (second) linear-recovery phase lasts shorter (because the alteration process happens fast), and more of the profile resembles the familiar square-root-of-time shape, indicative of a fixed wetting state.

The Role of Diffusion. The transport of reactive component is essential to alter the wettability and raise capillary forces that draw water into the matrix. In oil-wet and mixed-wet rocks, this relies heavily on molecular diffusion and, to some extent, dispersion after a phase flow has started. In the presented examples, the component was effectively taken into the matrix (see Fig. 10),

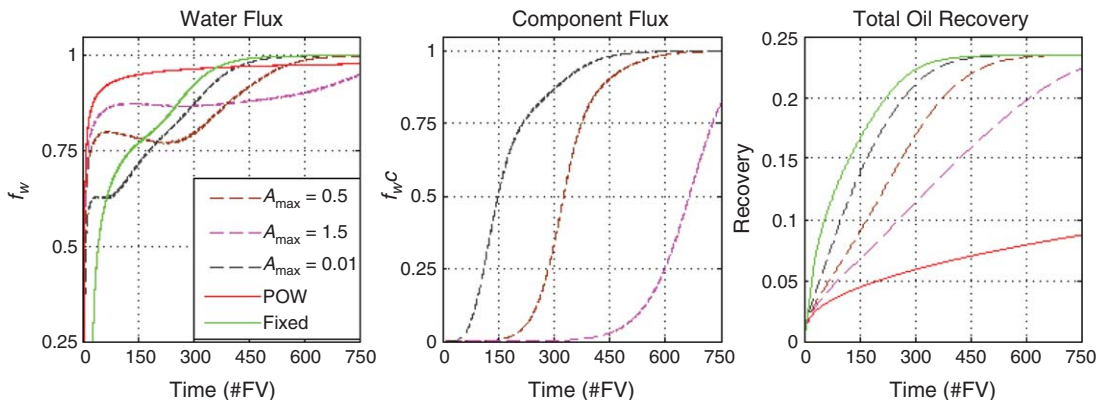


Fig. 13—Injected and produced water flux (left) and WA-agent flux f_w , $f_w c$ (middle) and oil recovery (right) for different values of A_{max} when $c = 1$. Cases are also compared with cases of fixed wettability corresponding to $c = 1$ or POW.

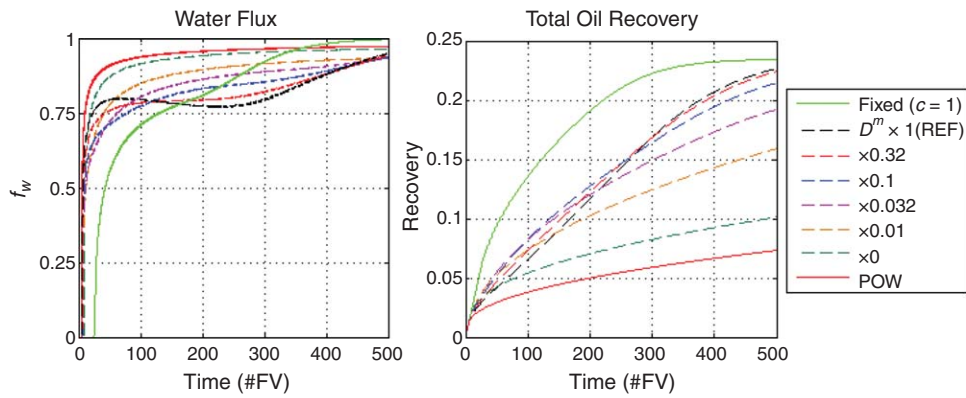


Fig. 14—Reference case ($c = 1$) with variation of the diffusion/dispersion term D^m (Eq. 15) by different factors. Slower transport of the WA agent reduces rate of recovery.

partly because the time scale of diffusion has been small (enough). To demonstrate how diffusion can limit the process, we have varied the matrix-diffusion term (Eq. 15) in Eq. 6 and Eq. 7 while keeping other parameters fixed. Results are presented in Figs. 14 and 15. Some component is brought in by imbibition, as seen by the increased recovery of the case $D^m \times 0$ compared with POW. Furthermore, recovery rate increases with the magnitude of the diffusion term. A surprising feature is that the cases with low diffusion have higher recovery at early times. One can explain this by the nonlinearity of the process in which WA is more effective at low concentrations (see Fig. 9). Therefore, it first appears beneficial that the WA agent is distributed along the flow path instead of advancing slower. For the long term, however, the lack of diffusive transport leads to production of the WA agent and less adsorption, meaning that it takes a longer time to obtain full recovery. Note that a square-root-of-time profile is more established at low-diffusion regimes, which agrees both with diffusion-like transport and slow imbibition.

Fig. 15 shows a distribution of water and WA agent after 250 FV was injected for different magnitudes of D^m . In the left figure, the WA agent is rapidly diffusing into the matrix, while water slowly imbibes. Moving right in the figure, WA agent diffuses slower. Water becomes limited by how fast the matrix wettability is altered, and the distributions of water and WA agent become

similar. Especially, we note that the uniform concentration profile along the fracture also produces a uniform imbibition profile.

Concluding Remarks

In this article, we have presented a 1D+1D model to illustrate how brine-dependent oil recovery by spontaneous imbibition (SI) may behave in a matrix/fracture system. Experiments have shown that SI is an important recovery mechanism in fractured reservoirs and that the ultimate recovery is controlled by wettability (Zhou et al. 2000; Graue et al. 2001; Haugen et al. 2010). It is possible to alter the wettability toward a more water-wet state and, hence, increase the potential for SI by introducing chemically reactive components (e.g., ions and chemicals) to the system (Hirasaki and Zhang 2004; Zhang and Austad 2006; Zhang et al. 2007; Ahsan et al. 2012). The matrix model could history match a brine-dependent SI experiment described in Zhang and Austad (2006). There is a need to understand how this behavior will appear on a larger scale, and our 1D+1D model gives an indication by considering this in a fracture/matrix flow context.

The model considers injection of water into a reservoir in which advective flow occurs in a fracture channel, whereas capillary flow appears in the matrix to feed the fracture with oil. The injected water carries a wettability-alteration (WA) agent that can

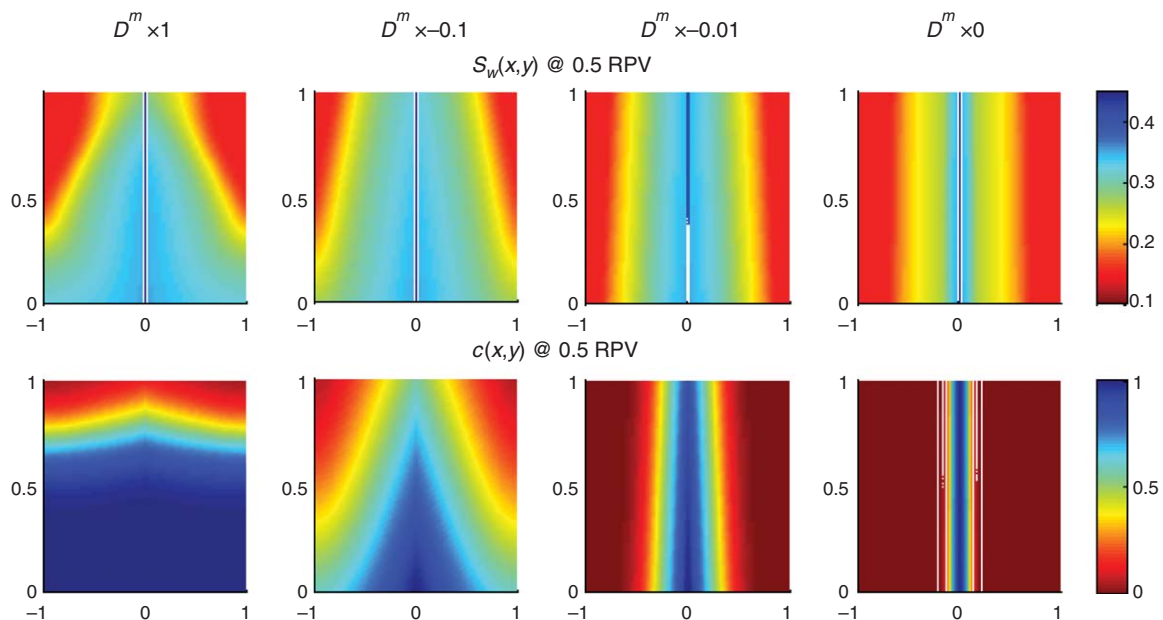


Fig. 15—Distributions of water (up) and component (down) after 0.5 RPV = 250 FV for different magnitudes of the diffusion term (Eq. 15).

enter the matrix, adsorb onto the rock surface, and alter the wettability toward a more-water-wet state. Darcy-scale modeling of WA requires proper knowledge of the geochemical interactions, represented by Eq. 13, and how they affect the saturation functions, represented by Eq. 14. Both factors may be time-dependent and may affect the efficiency of the recovery process. The numerical-solution procedure was validated by comparison with 2D simulations in ECLIPSE. The following observations were made:

- If the matrix wettability is fixed preferentially, oil-wet water breakthrough occurs quickly, and recovery is low. If the matrix is preferentially water-wet, the water breakthrough happens later, and recovery is higher. This behavior was seen experimentally in Haugen et al. (2010). At fixed wettability, the recovery from the given fracture/matrix geometry is linear before breakthrough and follows a square-root-of-time profile afterward, as discussed in Rangel-German and Kovscek (2002).
- The WA agent enters the matrix by SI of the water phase, dispersion, and diffusion. The dilution into connate water and adsorption onto the matrix rock delay the WA-agent breakthrough compared with the water front. A model for component transport in fractured reservoirs was also described in Geiger et al. (2013).
- Varying WA-agent concentrations also changes the amount of adsorption onto the rock. By linking WA to adsorption, it is therefore possible to explain differences in ultimate recovery when changing the concentration of the WA agent, as observed and discussed in Zhang and Austad (2006), Fernø et al. (2011), and Ahsan et al. (2012).
- The WA agent takes some time to enter the matrix, so the reservoir will initially behave as preferentially oil-wet (POW). This means that the time of water breakthrough will be similar to that of the POW reservoir. The SI of water and adsorption of WA agent change the capillary pressure in opposite directions (weaken or strengthen the driving force, respectively). If these mechanisms are of similar magnitude, this production stage can therefore be characterized by a linear recovery profile. If the diffusion process is slow, the distribution of WA agent limits the rate of recovery; see Fig. 14.
- One should not determine the effect of the WA agent by the breakthrough time, but by the behavior after breakthrough. It may be possible to see clear effects quickly because of the short residence time.
- The amount of WA agent that needs to adsorb to make a WA will also indicate how fast the alteration goes. If the amount is negligible, the alteration will follow the WA-agent front that lies ahead of the water front because of dispersion and diffusion. The matrix will then become preferentially water-wet at first contact with the imbibed water.
- If the matrix retains a large amount of WA agent by adsorption, the WA and recovery are controlled by the rate at which the WA agent is supplied to the reservoir. A linear profile in recovery develops that has a higher slope vs. time if less needs to adsorb.

Nomenclature

- a_1, a_2, b_1, k_1, k_2 = capillary pressure correlation parameters
 A = adsorbed WA agent
 A_{\max} = maximum adsorption of WA agent
 b = fracture half-width
 c = WA-agent concentration
 $c_{\text{imb}}, c_{\text{inj}}$ = imbibing or injected WA-agent concentration
 D_{mol} = molecular-diffusion coefficient
 D^i = dispersion coefficient
 f_{ji} = phase fractional-flow function
 J^i = scaled capillary pressure
 K^i = absolute permeability
 k_r^* = endpoint relative permeability
 k_{rj} = relative permeability
 L, E, T = relative permeability correlation parameters
 L_x = matrix width from fracture
 L_y = length of fracture

- P_c^i = capillary pressure
 r = adsorption-isotherm parameter
 S^* = normalized water saturation
 S_{jr} = residual saturation
 S_w = water saturation
 v_T^i = pore velocity
 w = relative adsorption of WA agent
 α^i = dispersivity
 β = pore-volume ratio
 λ_{ji} = phase mobility
 μ_i = viscosity
 ϕ^i = porosity

Note: indices $i = m, f$ (matrix, fracture) and $j = o, w$ (oil, water).

Acknowledgments

The research of Andersen has been supported by the National IOR Center of Norway.

References

- Agarwal, B., Hermansen, H., Sylte, J. E. et al. 2000. Reservoir Characterization of Ekofisk Field: A Giant, Fractured Chalk Reservoir in the Norwegian North Sea—History Match. *SPE Res Eval & Eng* **3** (6): 534–543. SPE-68096-PA. <http://dx.doi.org/10.2118/68096-PA>.
- Ahr, W. M. 2008. *Geology of Carbonate Reservoirs: The Identification, Description, and Characterization of Hydrocarbon Reservoirs in Carbonate Rocks*. Hoboken, New Jersey: Wiley.
- Ahsan, R., Madland, M. V., Bratteli, F. et al. 2012. A Study of Sulphate Ions—Effects on Aging and Imbibition Capillary Pressure Curve. Presented at the International Symposium of the Society of Core Analysts, Aberdeen, Scotland, UK, 27–30 August. SCA-2012-34.
- Akbar, M., Vissapragada, B., Alghamdi, A. et al. 2001. A Snapshot of Carbonate Reservoir Evaluation. *Oilfield Review* **12** (4): 20–41.
- Al-Hadhrami, H. S. and Blunt, M. J. 2001. Thermally Induced Wettability Alteration to Improve Oil Recovery in Fractured Reservoirs. *SPE Res Eval & Eng* **4**: 179–186. SPE-71866-PA. <http://dx.doi.org/10.2118/71866-PA>.
- Andersen, P. Ø. and Evje, S. 2012a. A Mathematical Model for Interpretation of Brine-Dependent Spontaneous Imbibition Experiments. Presented at ECMOR XIII, Biarritz, France. In *AIP Conference Proc.*, 2340–2343.
- Andersen, P. Ø. and Evje, S. 2012b. Two-Phase Flow in a Fissurized-Porous Media. In *AIP Conference Proc.*, 1479, 2340–2343.
- Andersen, P. Ø., Evje, S., Madland, M. V. et al. 2012. A Geochemical Model for Interpretation of Chalk Core Flooding Experiments. *Chemical Eng. Sci.* **84**: 218–241. <http://dx.doi.org/10.1016/j.ces.2012.08.038>.
- Anderson, W. G. 1987. Wettability Literature Survey—Part 4: Effects of Wettability on Capillary Pressure. *J Pet Technol* **39**: 1283–1300. SPE-15271-PA. <http://dx.doi.org/10.2118/15271-PA>.
- Appelo, C. A. J. and Postma, D. 2005. *Geochemistry, Groundwater and Pollution*. CRC Press Taylor & Francis Group.
- Aronofsky, J. S., Masse, L., and Natanson, S. G. 1958. A Model for the Mechanism of Oil Recovery From the Porous Matrix Due to Water Invasion in Fractured Reservoirs. *Petroleum Trans. AIME* **213**: 17–19.
- Austad, T., Strand, S., Madland, M. V. et al. 2008. Seawater in Chalk: An EOR and Compaction Fluid. *SPE Res Eval & Eng* **11**: 648–654. SPE-118431-PA. <http://dx.doi.org/10.2118/118431-PA>.
- Behbahani, H. and Blunt, M. J. 2004. Analysis of Imbibition in Mixed-Wet Rocks Using Pore-Scale Modeling. *SPE J.* **10**: 466–474. SPE-90132-PA. <http://dx.doi.org/10.2118/90132-PA>.
- Bourbiaux, B. J. 2009. Understanding the Oil Recovery Challenge of Water Drive Fractured Reservoirs. Presented at the International Petroleum Technology Conference, Doha, Qatar, 7–9 December. <http://dx.doi.org/10.2523/13909-MS>.
- Bourbiaux, B., Fournio, A., Nguyen, Q.-L. et al. 2014. Experimental and Numerical Assessment of Chemical EOR in Oil-Wet Naturally-Fractured Reservoirs. Presented at the SPE Improved Oil Recovery Symposium, Tulsa, Oklahoma, USA, 12–16 April. SPE-169140-MS. <http://dx.doi.org/10.2118/169140-MS>.

- Bourbiaux, B. J. and Kalaydjian, F. J. 1990. Experimental Study of Cocurrent and Countercurrent Flows in Natural Porous Media. *SPE Res Eng* **5**: 361–368. SPE-18283-PA. <http://dx.doi.org/10.2118/18283-PA>.
- Cai, J., Perfect, E., Cheng, C.-L. et al. 2014. Generalized Modeling of Spontaneous Imbibition Based on Hagen–Poiseuille Flow in Tortuous Capillaries With Variably Shaped Apertures. *Langmuir* **30**: 5142–5151. <http://dx.doi.org/10.1021/la5007204>.
- Chen, Z., Huan, G., and Ma, Y. 2006. *Computational Methods for Multiphase Flows in Porous Media*. Philadelphia, Pennsylvania: Society for Industrial and Applied Mathematics.
- Chilingar, G. V. and Yen, T. F. 1983. Some Notes on Wettability and Relative Permeabilities of Carbonate Reservoir Rocks, II. *Energy Sources* **7**: 67–75. <http://dx.doi.org/10.1080/00908318308908076>.
- Cuiec, L. 1984. Rock/Crude-Oil Interactions and Wettability: An Attempt To Understand Their Interrelation. Presented at the SPE Annual Technical Conference and Exhibition, Houston, Texas, USA, 16–19 September. SPE-13211-MS. <http://dx.doi.org/10.2118/13211-MS>.
- Dejam, M. and Hassanzadeh, H. 2011. Formation of Liquid Bridges Between Porous Matrix Blocks. *Aiche J.* **57**: 286–298. <http://dx.doi.org/10.1002/aic.12262>.
- De La Porte, J. J., Kossack, C. A., and Zimmerman, R. W. 2005. The Effect of Fracture Relative Permeabilities and Capillary Pressures on the Numerical Simulation of Naturally Fractured Reservoirs. SPE Annual Technical Conference and Exhibition, Dallas, Texas, USA, 9–12 October. SPE-95241-MS. <http://dx.doi.org/10.2118/95241-MS>.
- Delshad, M., Najafabadi, N. F., Anderson, G. A. et al. 2009. Modeling Wettability Alteration by Surfactants in Naturally Fractured Reservoirs. *SPE Res Eval & Eng* **12**: 361–370. SPE-100081-PA. <http://dx.doi.org/10.2118/100081-PA>.
- De Swaan, A. 1978. Theory of Waterflooding in Fractured Reservoirs. *SPE J.* **18**: 117–122. SPE-5892-PA. <http://dx.doi.org/10.2118/5892-PA>.
- Duijn, C. J., Molenaar, J., and Neef, M. J. 1995. The Effect of Capillary Forces on Immiscible Two-Phase Flow in Heterogeneous Porous Media. *Transport in Porous Media* **21**: 71–93. <http://dx.doi.org/10.1007/BF00615335>.
- Dullien, F. A. L. 1992. *Porous Media: Fluid Transport and Pore Structure*. San Diego, California: Academic Press.
- Evje, S. and Hiorth, A. 2011. A Model for Interpretation of Brine-Dependent Spontaneous Imbibition Experiments. *Advances in Water Resources* **34**: 1627–1642. <http://dx.doi.org/10.1016/j.advwatres.2011.09.003>.
- Fathi, S. J., Austad, T., and Strand, S. 2010. “Smart Water” As a Wettability Modifier in Chalk: The Effect of Salinity and Ionic Composition. *Energy & Fuels* **24**: 2514–2519. <http://dx.doi.org/10.1021/ef901304m>.
- Fathi, S. J., Austad, T., and Strand, S. 2011. Water-Based Enhanced Oil Recovery (EOR) by “Smart Water”: Optimal Ionic Composition for EOR in Carbonates. *Energy & Fuels* **25**: 5173–5179. <http://dx.doi.org/10.1021/ef201019k>.
- Fernø, M. A., Grønnsdal, R., Åsheim, J. et al. 2011. Use of Sulfate for Water-Based Enhanced Oil Recovery During Spontaneous Imbibition in Chalk. *Energy & Fuels* **25**: 1697–1706. <http://dx.doi.org/10.1021/ef200136w>.
- Gautam, P. S. and Mohanty, K. K. 2004. Matrix-Fracture Transfer Through Countercurrent Imbibition in Presence of Fracture Fluid Flow. *Transport in Porous Media* **55**: 309–337. <http://dx.doi.org/10.1023/B:TIPM.0000013326.95597.10>.
- Geiger, S., Dentz, M., and Neuweiler, I. 2013. A Novel Multi-Rate Dual-Porosity Model for Improved Simulation of Fractured and Multiporosity Reservoirs. *SPE J.* **18**: 670–684. SPE-148130-PA. <http://dx.doi.org/10.2118/148130-PA>.
- Golf-Racht, T. D. V. 1982. *Fundamentals of Fractured Reservoir Engineering*. Amsterdam: Elsevier.
- Graue, A., Bogno, T., Baldwin, B. A. et al. 2001. Wettability Effects on Oil-Recovery Mechanisms in Fractured Reservoirs. *SPE Res Eval & Eng* **4**: 455–466. SPE-74335-PA. <http://dx.doi.org/10.2118/74335-PA>.
- Gupta, R. and Mohanty, K. K. 2011. Wettability Alteration Mechanism for Oil Recovery From Fractured Carbonate Rocks. *Transport in Porous Media* **87**: 635–652. <http://dx.doi.org/10.1007/s11242-010-9706-5>.
- Haugen, A., Ferno, M. A., Bull, O. et al. 2010. Wettability Impacts on Oil Displacement in Large Fractured Carbonate Blocks. *Energy & Fuels* **24**: 3020–3027. <http://dx.doi.org/10.1021/ef1000453>.
- Haugen, A., Ferno, M. A., and Graue, A. 2007. Comparison of Numerical Simulations and Laboratory Waterfloods in Fractured Carbonates. Presented at the SPE Annual Technical Conference and Exhibition, Anaheim, California, USA, 11–14 November. SPE-110368-MS. <http://dx.doi.org/10.2118/110368-MS>.
- Haugen, A., Ferno, M. A., and Graue, A. 2008. Numerical Simulation and Sensitivity Analysis of In-Situ Fluid Flow in MRI Laboratory Waterfloods of Fractured Carbonate Rocks at Different Wettabilities. Presented at the SPE Annual Technical Conference and Exhibition, Denver, Colorado, USA, 21–24 September. SPE-116145-MS. <http://dx.doi.org/116145-MS>.
- Haugen, Å., Fernø, M. A., Mason, G. et al. 2014. Capillary Pressure and Relative Permeability Estimated From a Single Spontaneous Imbibition Test. *J. Petrol. Sci. & Eng.* **115**: 66–77. <http://dx.doi.org/10.1016/j.petrol.2014.02.001>.
- Hiorth, A., Cathles, L. M., and Madland, M. V. 2010. The Impact of Pore Water Chemistry on Carbonate Surface Charge and Oil Wettability. *Transport in Porous Media* **85**: 1–21. <http://dx.doi.org/10.1007/s11242-010-9543-6>.
- Hirasaki, G. and Zhang, D. L. 2004. Surface Chemistry of Oil Recovery From Fractured, Oil-Wet, Carbonate Formations. *SPE J.* **9**: 151–162. SPE-88365-PA. <http://dx.doi.org/10.2118/88365-PA>.
- Karimi, A., Fakhroueian, Z., Bahramian, A. et al. 2012. Wettability Alteration in Carbonates Using Zirconium Oxide Nanofluids: EOR Implications. *Energy & Fuels* **26**: 1028–1036. <http://dx.doi.org/10.1021/ef201475u>.
- Kazemi, H., Merrill Jr., L. S., Porterfield, K. L. et al. 1976. Numerical Simulation of Water-Oil Flow in Naturally Fractured Reservoirs. *SPE J.* **16**: 317–326. SPE-5719-PA. <http://dx.doi.org/10.2118/5719-PA>.
- LeVeque, R. J. 2002. *Finite Volume Methods for Hyperbolic Problems*, volume 31. Cambridge, UK: Cambridge University Press.
- Li, K. 2007. Scaling of Spontaneous Imbibition Data With Wettability Included. *J. Contaminant Hydrology* **89**: 218–230. <http://dx.doi.org/10.1016/j.jconhyd.2006.09.009>.
- Lomeland, F., Ebeltoft, E., and Thomas, W. H. 2005. A New Versatile Relative Permeability Correlation. Presented at the International Symposium of the Society of Core Analysts, Toronto, Canada.
- Ma, S., Morrow, N. R., and Zhang, X. 1997. Generalized Scaling of Spontaneous Imbibition Data for Strongly Water-Wet Systems. *J. Petrol. Sci. & Eng.* **18** (3–4): 165–178. [http://dx.doi.org/10.1016/S0920-4105\(97\)00020-X](http://dx.doi.org/10.1016/S0920-4105(97)00020-X).
- Mainguy, M. and Ulm, F. J. 2001. Coupled Diffusion-Dissolution Around a Fracture Channel: The Solute Congestion Phenomenon. *Transport in Porous Media* **45**: 479–495. <http://dx.doi.org/10.1023/A:1012096014084>.
- Mattax, C. C. and Kyte, J. R. 1962. Imbibition Oil Recovery From Fractured, Water-Drive Reservoir. *SPE J.* **2**: 177–184. SPE-187-PA. <http://dx.doi.org/10.2118/187-PA>.
- McWhorter, D. B. and Sunada, D. K. 1990. Exact Integral Solutions for Two-Phase Flow. *Water Resources Research* **26**: 399–413. <http://dx.doi.org/10.1029/WR026i003p00399>.
- Megawati, M., Hiorth, A., and Madland, M. V. 2012. The Impact of Surface Charge on the Mechanical Behavior of High-Porosity Chalk. *Rock Mechanics and Rock Eng.* **46**: 1073–1090. <http://dx.doi.org/10.1007/s00603-012-0317-z>.
- Mirzaei-Paiaman, A., Masihi, M., and Standnes, D. C. 2011. An Analytic Solution for the Frontal Flow Period in 1D Counter-Current Spontaneous Imbibition Into Fractured Porous Media Including Gravity and Wettability Effects. *Transport in Porous Media* **89**: 49–62. <http://dx.doi.org/10.1007/s11242-011-9751-8>.
- Nelson, R. A. 2001. *Geologic Analysis of Naturally Fractured Reservoirs*. Boston, Massachusetts: Gulf Professional Publishers.
- Pooladi-Darvish, M. and Firoozabadi, A. 2000a. Cocurrent and Countercurrent Imbibition in a Water-Wet Matrix Block. *SPE J.* **5**: 3–11. SPE-38443-PA. <http://dx.doi.org/10.2118/38443-PA>.
- Pooladi-Darvish, M. and Firoozabadi, A. 2000b. Experiments and Modeling of Water Injection in Water-Wet Fractured Porous Media. *J. Can Pet Technol* **39**: 31–42. SPE-00-03-02-PA. <http://dx.doi.org/10.2118/00-03-02-PA>.
- Qiao, C., Li, L., Johns, R. T. et al. 2014. A Mechanistic Model for Wettability Alteration by Chemically Tuned Water Flooding in Carbonate

Reservoirs. Presented at the SPE Annual Technical Conference and Exhibition, Amsterdam, The Netherlands, 27–29 October. SPE-170966-MS. <http://dx.doi.org/10.2118/170966-MS>.

Rangel-German, E. R. and Kovscek, A. R. 2002. Experimental and Analytical Study of Multidimensional Imbibition in Fractured Porous Media. *J. Petrol. Sci. & Eng.* **36**: 45–60. [http://dx.doi.org/10.1016/S0920-4105\(02\)00250-4](http://dx.doi.org/10.1016/S0920-4105(02)00250-4).

Rao, D. N. 1999. Wettability Effects in Thermal Recovery Operations. *SPE Res Eval & Eng* **2**: 420–430. SPE-57897-PA. <http://dx.doi.org/10.2118/57897-PA>.

Roehl, P. O. and Choquette, P. W. 1985. *Carbonate Petroleum Reservoirs*. New York: Springer.

Salimi, H. and Bruining, J. 2011. The Influence of Heterogeneity, Wetting, and Viscosity Ratio on Oil Recovery From Vertically Fractured Reservoirs. *SPE J.* **16**: 411–428. SPE-140152-PA. <http://dx.doi.org/10.2118/140152-PA>.

Schmid, K. S. and Geiger, S. 2012. Universal Scaling of Spontaneous Imbibition for Water-Wet Systems. *Water Resources Research* **48**: W03507. <http://dx.doi.org/10.1029/2011WR011566>,

Schmid, K. S. and Geiger, S. 2013. Universal Scaling of Spontaneous Imbibition for Arbitrary Petrophysical Properties: Water-Wet and Mixed-Wet States and Handy's Conjecture. *J. Petrol. Sci. & Eng.* **101**: 44–61. <http://dx.doi.org/10.1016/j.petrol.2012.11.015>.

Skjæveland, S. M., Siqveland, L. M., Kjosavik, A. et al. 2000. Capillary Pressure Correlation for Mixed-Wet Reservoirs. *SPE Res Eval & Eng* **3**: 60–67. SPE-60900-PA. <http://dx.doi.org/10.2118/60900-PA>.

Stoll, M., Hofman, J., Ligthelm, D. J. et al. 2008. Toward Field-Scale Wettability Modification—The Limitations of Diffusive Transport. *SPE Res Eval & Eng* **11**: 633–640. SPE-107095-PA. <http://dx.doi.org/10.2118/107095-PA>.

Strand, S., Standnes, D. C., and Austad, T. 2003. Spontaneous Imbibition of Aqueous Surfactant Solutions Into Neutral to Oil-Wet Carbonate Cores: Effects of Brine Salinity and Composition. *Energy & Fuels* **17**: 1133–1144. <http://dx.doi.org/10.1021/ef030051s>.

Strand, S., Standnes, D. C., and Austad, T. 2006. New Wettability Test for Chalk Based on Chromatographic Separation of SCN⁻ and SO₄²⁻. *J. Petrol. Sci. & Eng.* **52**: 187–197. <http://dx.doi.org/10.1016/j.petrol.2006.03.021>.

Tavassoli, Z., Zimmerman, R., and Blunt, M. 2005. Analytic Analysis for Oil Recovery During Counter-Current Imbibition in Strongly Water-Wet Systems. *Transport in Porous Media* **58**: 173–189. <http://dx.doi.org/10.1007/s11242-004-5474-4>.

Terez, I. E. T. and Firoozabadi, A. 1999. Water Injection in Water-Wet Fractured Porous Media: Experiments and a New Model With Modified Buckley–Leverett Theory. *SPE J.* **4**: 134–141. SPE-56854-PA. <http://dx.doi.org/10.2118/56854-PA>.

Treiber, L. E. and Owens, W. W. 1972. A Laboratory Evaluation of the Wettability of Fifty Oil-Producing Reservoirs. *SPE J.* **12**: 531–540. SPE-3526-PA. <http://dx.doi.org/10.2118/3526-PA>.

Unsal, E., Matthai, S. K., and Blunt, M. J. 2010. Simulation of Multiphase Flow in Fractured Reservoirs Using a Fracture-Only Model With Transfer Functions. *Computational Geosci.* **14**: 527–538. <http://dx.doi.org/10.1007/s10596-009-9168-4>.

Xie, X., Weiss, W. W., Tong, Z. J. et al. 2005. Improved Oil Recovery From Carbonate Reservoirs by Chemical Stimulation. *SPE J.* **10**: 276–285. SPE-89424-PA. <http://dx.doi.org/10.2118/89424-PA>.

Yu, L., Evje, S., Kleppe, H. et al. 2009. Spontaneous Imbibition of Seawater Into Preferentially Oil-Wet Chalk Cores—Experiments and Simulations. *J. Petrol. Sci. & Eng.* **66**: 171–179. <http://dx.doi.org/10.1016/j.petrol.2009.02.008>.

Yu, L. P., Kleppe, H., Kaarstad, T. et al. 2008. Modelling of Wettability Alteration Processes in Carbonate Oil Reservoirs. *Networks and Heterogeneous Media* **3**: 149–183.

Yu, L., Standnes, D. C., and Skjæveland, S. M. 2007. Wettability Alteration of Chalk by Sulphate Containing Water, Monitored by Contact Angle Measurement. Presented at the International Symposium of the Society of Core Analysts, Calgary, Canada.

Zhang, P. M. and Austad, T. 2006. Wettability and Oil Recovery From Carbonates: Effects of Temperature and Potential Determining Ions. *Colloids and Surfaces A: Physicochemical and Engineering Aspects* **279**: 179–187. <http://dx.doi.org/10.1016/j.colsurfa.2006.01.009>.

Zhang, P., Tweheyo, M. T., and Austad, T. 2007. Wettability Alteration and Improved Oil Recovery by Spontaneous Imbibition of Seawater Into Chalk: Impact of the Potential Determining Ions Ca²⁺, Mg²⁺, and SO₄²⁻. *Colloids and Surfaces A: Physicochemical and Engineering Aspects* **301**: 199–208. <http://dx.doi.org/10.1016/j.colsurfa.2006.12.058>.

Zhou, D., Jia, L., Kamath, J. et al. 2002. Scaling of Counter-Current Imbibition Processes in Low-Permeability Porous Media. *J. Petrol. Sci. & Eng.* **33**: 61–74. [http://dx.doi.org/10.1016/S0920-4105\(01\)00176-0](http://dx.doi.org/10.1016/S0920-4105(01)00176-0).

Zhou, X., Morrow, N. R., and Ma, S. 2000. Interrelationship of Wettability, Initial Water Saturation, Aging Time, and Oil Recovery by Spontaneous Imbibition and Waterflooding. *SPE J.* **5**: 199–207. SPE-62507-PA. <http://dx.doi.org/10.2118/62507-PA>.

Appendix A

Recovery. Recovery is calculated on the basis of recovered oil compared with initial oil in place:

$$R = \frac{\beta(\bar{S}_w^m - S_{w,0}^m) + (\bar{S}_w^f - S_{w,0}^f)}{\beta(1 - S_{w,0}^m) + (1 - S_{w,0}^f)} \quad (\text{A-1})$$

\bar{S}_w^m , \bar{S}_w^f represent average saturations in matrix and fracture, respectively, and $\beta = \frac{L_x \phi^m}{b \phi^f}$ represents the ratio of matrix pore volume to fracture pore volume. If the fracture is fully flooded and the matrix can obtain a saturation $S_{w,eq}^m$ such that $P_c(S_{w,eq}^m) = 0$, the maximum recovery will be

$$R_{\max} = \frac{\beta(S_{w,eq}^m - S_{w,0}^m) + (1 - S_{w,0}^f)}{\beta(1 - S_{w,0}^m) + (1 - S_{w,0}^f)} \quad (\text{A-2})$$

Operator Splitting. The mathematical solution of Eqs. 6 and 7 is implemented with an operator-splitting approach. This provides control on stability for each system and also gives flexibility if more-advanced features are included. We solve the three following systems separately:

(a) Advection in the fracture (no changes in the matrix),

$$\begin{aligned} \phi^f \partial_t S_w + \phi^f v_T^f \partial_y (f_w^f) &= 0 \\ \phi^f \partial_t (S_w c) + \phi^f v_T^f \partial_y (f_w^f c) &= 0. \end{aligned} \quad (x, y) \in \Omega^f \quad (\text{A-3})$$

(b) Spontaneous imbibition along matrix without component dispersion/diffusion,

$$\begin{aligned} \phi^m \partial_t S_w &= -\partial_x (\lambda_o^m f_w^m K^m \partial_x P_c^m) \\ \phi^m \partial_t (S_w c + A) &= -\partial_x (\lambda_o^m f_w^m K^m c \partial_x P_c^m) \\ \phi^f \partial_t S_w &= -\frac{1}{b} (K \lambda_{ofw} \partial_x P_c) |_{\{x=0^+\}} \\ \phi^f \partial_t (S_w c) &= -\frac{1}{b} (K \lambda_{ofw} c \partial_x P_c) |_{\{x=0^+\}} \end{aligned} \quad (x, y) \in \Omega^m \quad (\text{A-4})$$

(c) Component dispersion/diffusion along matrix,

$$\begin{aligned} \phi^m \partial_t (S_w c + A) &= \phi^m \partial_x (S_w D^m \partial_x c), \\ \phi^f \partial_t (S_w c) &= \frac{1}{b} (\phi S_w D \partial_x c) |_{\{x=0^+\}} \end{aligned} \quad (x, y) \in \Omega^m \quad (\text{A-5})$$

For each splitting step dT , advection (Eq. A-3) is carried out for $dT/2$, followed by SI (Eq. A-4) and dispersion (Eq. A-5) interchanging (every local timestep of imbibition) until a full splitting step dT is completed. Then, advection (Eq. A-3) is again performed over a time $dT/2$.

Discretization. (a) Advection in fracture: The system of Eq. A-3 is solved explicitly with the discretization that follows:

$$\begin{aligned} \frac{S_i^{n+1} - S_i^n}{\Delta t} + v_T \frac{f_{i+1/2}^n - f_{i-1/2}^n}{\Delta y} &= 0 \\ \frac{m_i^{n+1} - m_i^n}{\Delta t} + v_T \frac{f_{i+1/2}^n c_i^n - f_{i-1/2}^n c_{i-1}^n}{\Delta y} &= 0 \end{aligned} \quad (i = 1 : N_y),$$

where the van Leer slope limiter is used to provide second-order accuracy of the advective terms in y with the ‘‘Monotonic Upstream-Centered Scheme for Conservation Laws’’ (LeVeque 2002),

$$\begin{aligned} f_{i+1/2} &= 1/2 \left(f_i + \nu^{1/2} s_i + \frac{\Delta y}{2} \sigma_i^+ \right) \\ &\quad + 1/2 \left(f_{i+1} + \nu^{1/2} s_{i+1} - \frac{\Delta y}{2} \sigma_{i+1}^- \right), \\ \sigma_i^+ &= \sigma \left(\delta f_{i-1/2}^+, \delta f_{i+1/2}^+ \right), \sigma_i^- = \sigma \left(\delta f_{i+1/2}^-, \delta f_{i+3/2}^- \right), \\ \sigma(u, v) &= \frac{\text{sgn}(u) + \text{sgn}(v)}{2} \frac{2uv}{u+v}, \\ \delta f_{i+1/2}^+ &= \frac{1}{\Delta y} \left[(f_{i+1} + \nu^{1/2} s_{i+1}) - (f_i + \nu^{1/2} s_i) \right], \\ \delta f_{i+1/2}^- &= \frac{1}{\Delta y} \left[(f_{i+1} - \nu^{1/2} s_{i+1}) - (f_i - \nu^{1/2} s_i) \right]. \end{aligned}$$

For stability, we select $\nu^{1/2} = \sup_s |f'|$ and timestep such that $\sup_s |f'| v_T \frac{\Delta t}{\Delta y} = 0.5$.

(b) SI: The system of Eq. A-4 is discretized explicitly as follows:

$$\begin{aligned} \phi^f \frac{S_1^{n+1} - S_1^n}{\Delta t} &= -\frac{1}{b} K(\lambda_{ofw})_{3/2}^n \frac{P_2^n - P_1^n}{2\Delta x}, \\ \phi^f \frac{m_1^{n+1} - m_1^n}{\Delta t} &= -\frac{1}{b} K(\lambda_{ofw} c)_{3/2}^n \frac{P_2^n - P_1^n}{2\Delta x}, \\ \phi^m \frac{S_i^{n+1} - S_i^n}{\Delta t} &= -\frac{1}{\Delta x} \\ &\quad \times \left[K(\lambda_{ofw})_{i+1/2}^n \frac{P_{i+1}^n - P_i^n}{\Delta x} - K(\lambda_{ofw})_{i-1/2}^n \frac{P_i^n - P_{i-1}^n}{\Delta x} \right], \\ \phi^m \frac{m_i^{n+1} - m_i^n}{\Delta t} &= -\frac{1}{\Delta x} \\ &\quad \times \left[K(\lambda_{ofw} c)_{i+1/2}^n \frac{P_{i+1}^n - P_i^n}{\Delta x} - K(\lambda_{ofw} c)_{i-1/2}^n \frac{P_i^n - P_{i-1}^n}{\Delta x} \right]. \end{aligned} \quad (i = 3 : N_x)$$

Cell 1 denotes the fracture, whereas Cell $2:N_x+1$ are matrix cells starting next to the fracture and ending at the boundary. P_i denotes capillary pressure P_c in cell i . Cell 1 uses a flux on the basis of knowing the capillary pressure at the interface. Cell 2 uses a left flux consistent with Cell 1 and a right flux consistent with Cell 3. Cell N_x+1 has a closed outer boundary (zero flux). We use an upwind formulation on the coefficients:

$$\begin{aligned} (\lambda_{ofw})_{i+1/2} &= (\lambda_o)_{i+1/2} \max[0, \text{sgn}(P_{i+1} - P_i)] \\ &\quad + (\lambda_o)_{i+1/2} \max[0, -\text{sgn}(P_{i+1} - P_i)] \\ (\lambda_{ofw} c)_{i+1/2} &= (\lambda_o)_{i+1/2} c_i \max[0, \text{sgn}(P_{i+1} - P_i)] \\ &\quad + (\lambda_o)_{i+1/2} c_{i+1} \max[0, -\text{sgn}(P_{i+1} - P_i)]. \end{aligned}$$

For stability, we require that the change in capillary pressure in a given cell is less than half the difference to its neighbors. For the fracture cell, the limitation on the timestep is set so that the saturation remains nonnegative.

(c) Dispersion/diffusion along matrix: Discretization of the system of Eq. A-5 is made with a fully implicit solver. Let $m_i^n = V_i^n c_i^n$ such that

$$\begin{aligned} V_1^n &= S_1^n, & (i = 1) \\ V_i^n &= S_i^n + A_{\max} \frac{r}{1 + r c_i^n}, & (i = 2 : N_x + 1). \end{aligned}$$

The system of equations that we solve can be written as

$$\begin{aligned} \phi^f \frac{V_1^{n+1} c_1^{n+1} - V_1^n c_1^n}{\Delta t} &= \frac{1}{b} (\phi SD)_{3/2} \frac{c_2^{n+1} - c_1^{n+1}}{2\Delta x}, \quad (i = 1) \\ \frac{V_i^{n+1} c_i^{n+1} - V_i^n c_i^n}{\Delta t} &= \\ \frac{1}{\Delta x} \left[(SD)_{i+1/2} \frac{c_{i+1}^{n+1} - c_i^{n+1}}{\Delta x} - (SD)_{i-1/2} \frac{c_i^{n+1} - c_{i-1}^{n+1}}{\Delta x} \right], & (i = 3 : N_x + 1) \end{aligned}$$

Again, we note that Cell 1 bases its gradient on the value at the interface. Cell 2 and N_x+1 are treated similarly, as described for the system of Eq. A-4. Assuming V_i does not change much from one timestep to the next, we initially approximate $V_i^{n+1} \approx V_i^n$ to obtain a linear system of equations. The system can be written in tridiagonal form and solved with LU-factorization [see a description in Chen et al. (2006)]. With the new concentrations $c_{i^{n+1}}$, we update $V_{i^{n+1}}$ and iterate until convergence.

Pål Ø. Andersen is a post-doctorate researcher at the University of Stavanger (UoS). He holds an MSc degree in reservoir technology and a PhD degree in petroleum technology, both from UoS. Andersen’s research interests include core-scale modeling, upscaling, enhanced oil recovery (EOR), and fractured reservoirs.

Steinar Evje is a professor in applied mathematics and is currently working in the Department of Petroleum Engineering, UoS. He is working on various multiphase models relevant for wellbore operations and porous-media flow (reservoir flow). Evje holds a PhD degree in applied mathematics from the University of Bergen, Norway.

Hans Kleppe has been a professor at UoS for more than 25 years. His current research interest is reservoir simulation including history matching, optimization, upscaling, and modeling of wettability-alteration processes. Kleppe has authored or coauthored more than 15 technical papers. He holds a PhD degree in mathematics from the Massachusetts Institute of Technology.

Svein M. Skjæveland is a professor of reservoir engineering and Director of Academia with the National IOR Centre of Norway at the UoS. He holds a PhD degree from the Norwegian University of Science and Technology in engineering physics and a PhD degree in petroleum engineering from Texas A&M University.